

# **Automatic Detection and Classification of Scoliosis from Spine X-rays using Transfer Learning**



Author

Arslan Amin

NUST 00000319267

Supervisor

Dr. Muhammad Usman Akram

DEPARTMENT OF COMPUTER & SOFTWARE ENGINEERING  
COLLEGE OF ELECTRICAL & MECHANICAL ENGINEERING  
NATIONAL UNIVERSITY OF SCIENCES AND TECHNOLOGY

ISLAMABAD

September 2022

Automatic Detection and Classification of Scoliosis from Spine X-  
rays using Transfer Learning

Author

Arslan Amin

NUST 00000319267

A thesis submitted in partial fulfillment of the requirements for the degree of  
MS Computer and Software Engineering

Thesis Supervisor

Dr. Muhammad Usman Akram

Thesis Supervisor's Signature: \_\_\_\_\_

DEPARTMENT OF COMPUTER & SOFTWARE ENGINEERING  
COLLEGE OF ELECTRICAL & MECHANICAL ENGINEERING  
NATIONAL UNIVERSITY OF SCIENCES AND TECHNOLOGY,

ISLAMABAD

September 2022

## **Declaration**

I attest that I am the author of the research paper titled "*Automatic Detection and Classification of Scoliosis from Spine X-rays Using Transfer Learning*." The work hasn't been submitted anywhere else for review. The use of the content from other sources has been appropriately acknowledged.

Signature of Student

Arslan Amin

NUST 00000319267

## **Language Correctness Certificate**

An English expert has proofread this thesis, and it is error-free in terms of spelling, grammar, syntax, semantics, and typing. In addition, the thesis follows the guidelines provided by the university.

Signature of Student

Arslan Amin

NUST 00000319267

Signature of Supervisor

Dr. Muhammad Usman Akram

## **Copyright Statement**

- Copyright in the text of this thesis rests with the student author. Copies (by any process) either in full or of extracts, may be made only by instructions given by the author and lodged in the Library of NUST College of E&ME. Details may be obtained by the Librarian. This page must form part of any such copies made. Further copies (by any process) may not be made without permission (in writing).
- The ownership of any intellectual property rights which may be described in this thesis is vested in NUST College of E&ME, subject to any prior agreement to the contrary, and may not be made available for use by third parties without the written permission of the College of E&ME, which will prescribe the terms and conditions of any such agreement.
- Further information on the conditions under which disclosures and exploitation may take place is available from the Library of NUST College of E&ME, Rawalpindi.

## **Acknowledgments**

In the name of Allah, the Most Gracious and Merciful, who has been my source of strength, wisdom, and the capacity for understanding throughout my life. I am appreciative to Allah, the Almighty, for giving me the ability to finish my research quickly. Nothing will occur without Allah's assistance.

I want to express my gratitude to my parents for their unwavering support in all aspects of my life. Without the prayers of my parents, whose support and wisdom I rely on in everything I do, I would be nothing. They serve as the best possible role models. My beloved brothers, who were at my side through thick and thin, continued to assist me in every area of my life even though I was unable to walk.

I want to sincerely thank my mentor, Dr. Muhammad Usman Akram, for his patient mentoring, contagious enthusiasm, and helpful criticism of my research project. I consider myself fortunate to have such a helpful advisor and gracious mentor for my research.

I also want to express my gratitude to my colleague Mr. Moneeb Abbas, whose experience and insight was very helpful to the research.

Finally, I want to thank all of my friends and the people who have supported and encouraged me throughout my research.

*Dedicated to my father, **Mr. Muhammad Amin**, and my dear brothers, whose unwavering support and collaboration helped me achieve this goal.*

## Abstract

In the last few years, the data is increasing in healthcare day by day. A manual system cannot reach to handle this big amount of data. An AI approach is organized to detect different features of medical data with an accurate diagnosis of multiple diseases. This research work provides Automatic detection and classification of Scoliosis (ADCS) using X-ray images. The spine of a patient with scoliosis curves in an S- or C-pattern, which is a pattern in opposite directions. The spine bends while rotating and curls sideways, causing this three-dimensional abnormality. X-ray imaging is used to identify scoliosis; however, it has historically been difficult and time-consuming for the lumbar, cervical, and thoracic spinal structures. The manual approach to calculating spine curvature gave poor results with the lowest degree of precision. The status of the spine's vertebrae must be accurately determined from medical images for several clinical uses of spinal x-rays imaging. It happens when noisy or irrelevant material occurs in spinal x-rays images, it calculates curvature to be inappropriate. This research proposed an automated framework (ADCS) for detecting the curvature of the spine from the spinal column. According to the increase of a large amount of data in medical departments, deep learning models provide useful information from the images already gathered in primary care. Deep learning algorithms offer a quicker and more effective scoliosis identification method than manual X-ray analysis. Using a pre-trained EfficientNet (EN) model, scoliosis is detected and classified from X-ray images of spine curvature. In the first step, we attained an accuracy of 76% in the initial evaluation of the model without augmentation. In the second step, we used the augmentation technique with the same model and as a result, we were able to attain an accuracy of 89%. Our results show that spine curvature from spine x-rays may be detected and classified using the automatic scoliosis detection techniques that have been proposed.

**Keywords:** *Spinal Cord, Vertebrae, Scoliosis, Deep learning, EfficientNet, Classification, Transfer learning, Computer service diagnostic, X-rays images. Data augmentation*



## Table of Contents

<b>DECLARATION.....</b>	<b>I</b>
<b>LANGUAGE CORRECTNESS CERTIFICATE.....</b>	<b>II</b>
<b>COPYRIGHT STATEMENT.....</b>	<b>III</b>
<b>ACKNOWLEDGMENTS .....</b>	<b>IV</b>
<b>ABSTRACT.....</b>	<b>VI</b>
<b>LIST OF FIGURES .....</b>	<b>X</b>
<b>LIST OF TABLES .....</b>	<b>XI</b>
<b>CHAPTER 1: INTRODUCTION.....</b>	<b>1</b>
1.1    MOTIVATION.....	2
1.2    PROBLEM STATEMENT .....	2
1.3    AIMS AND OBJECTIVES .....	2
1.4    STRUCTURE OF THESIS.....	3
<b>CHAPTER 2: SPINE CURVATURE AND ITS DISEASES.....</b>	<b>4</b>
2.1    ANATOMY OF SPINE.....	4
2.1.1 <i>Cervical Spine</i> .....	5
2.1.2 <i>Thoracic Spine</i> .....	5
2.1.3 <i>Lumbar Spine</i> .....	6
2.1.4 <i>Sacrum</i> .....	6
2.1.5 <i>Coccyx</i> .....	6
2.2    INTERVERTEBRAL DISCS .....	6
2.3    WHAT IS SCOLIOSIS AND ITS TYPES?.....	7
2.3.1 <i>Different types of Scoliosis</i> .....	7
2.4    DIFFERENT SHAPES OF SCOLIOSIS.....	8
2.4.1 <i>Normal Curve</i> .....	8
2.4.2 <i>S-Shaped Curve</i> .....	9
2.4.3 <i>C-Shaped Curve</i> .....	10
2.4.4 <i>Causes</i> .....	11
2.4.4 <i>Risks Factors</i> .....	11
2.4.5 <i>Complications</i> .....	11

2.5	METHODS AND TECHNOLOGIES USED FOR DIAGNOSING THE SCOLIOSIS.....	12
2.5.1	<i>Method and Technique for Assessment of Scoliosis using radiography.....</i>	12
2.5.2	<i>Method and Technique for Assessment of Scoliosis using Magnetic Resonance Imaging (MRI) .....</i>	12
2.5.3	<i>Computer Tomography (CT) .....</i>	12
2.5.4	<i>Ultrasound .....</i>	12
2.6	TREATMENT OF SCOLIOSIS.....	13
2.6.1	<i>Braces .....</i>	13
2.6.2	<i>Surgery.....</i>	14
2.7	EXERCISES FOR SCOLIOSIS .....	14
2.7.1	<i>Individual therapy of Scoliosis.....</i>	14
2.7.2	<i>Spine Core method.....</i>	14
2.7.3	<i>Lyon approach .....</i>	15
2.7.3	<i>Dobomed physical therapy .....</i>	15
2.7.4	<i>Barcelona physical therapy .....</i>	15
2.7.5	<i>Scientific exercise for scoliosis .....</i>	15
2.7.6	<i>Schroth method .....</i>	15
2.8	OTHER DISEASES OF SPINAL DEFORMITY .....	15
2.8.1	<i>Kyphosis.....</i>	15
2.8.2	<i>Lordosis.....</i>	16
<b>CHAPTER 3: LITERATURE REVIEW .....</b>		<b>18</b>
3.1	DATA AUGMENTATION .....	18
3.2	CLASSIFICATION .....	21
<b>RESEARCH GAP .....</b>		<b>28</b>
<b>CHAPTER 4: PROPOSED METHODOLOGY.....</b>		<b>29</b>
4.1	CLASSIFICATION .....	29
4.2	DATA AUGMENTATION .....	30
4.3	EFFICIENTNET MODEL B4 .....	31
4.3.1	<i>Compound Scaling .....</i>	32
4.3.2	<i>Working of EfficientNet.....</i>	33
4.3.3	<i>EfficientNet's architecture with MBCConv .....</i>	34
4.3.4	<i>ImageNet results for EfficientNet.....</i>	35

4.3.5	<i>Results of Transfer Learning for EfficientNet</i> .....	35
4.4	GAP LAYER (GLOBAL AVERAGE POOLING) .....	36
4.5	SOFTMAX ACTIVATION LAYER.....	36
4.6	LOSS FUNCTION .....	37
4.6.1	<i>Sparse Categorical Cross Entropy</i> .....	37
4.7	OPTIMIZER .....	38
4.7	TRANSFER LEARNING.....	39
4.8	PIPELINE AND EXPERIMENTAL SETUP .....	40
<b>CHAPTER 5:</b>	<b>EXPERIMENTAL RESULTS</b> .....	<b>42</b>
5.1	DATASET.....	42
5.1.1	<i>AASCE 2019 Dataset</i> .....	42
5.2	PERFORMANCE EVALUATION .....	43
5.2	RESULTS .....	44
5.2.1	<i>Results of the EfficientNet model's classification without augmentation</i> .....	44
5.2.2	<i>Results of the EfficientNet model's classification with augmentation</i> .....	45
5.2.3	<i>Classification Accuracy with and without Augmentation</i> .....	46
<b>DISCUSSION</b>	.....	<b>48</b>
<b>CHAPTER 6:</b>	<b>CONCLUSION AND FUTURE WORK</b> .....	<b>49</b>
6.1	CONCLUSION.....	49
6.2	CONTRIBUTION .....	49
6.2	FUTURE WORK.....	50
<b>REFERENCES</b>	.....	<b>51</b>

## List of Figures

<b>Figure 1:</b> Anatomy of Spine [11] .....	5
<b>Figure 2:</b> Intervertebral Discs .....	7
<b>Figure 3:</b> Normal Curve .....	9
<b>Figure 4:</b> S-Shaped Curve .....	10
<b>Figure 5:</b> C-Shaped Curve .....	10
<b>Figure 6:</b> Methods for Analyzing Scoliosis .....	13
<b>Figure 7:</b> Comparison of Scoliosis, Kyphosis, and Lordosis.....	16
<b>Figure 8:</b> Abstract Level Diagram of Classification.....	29
<b>Figure 9:</b> Spinal Augmented x-rays images.....	30
<b>Figure 10:</b> Compound Scaling [45] .....	32
<b>Figure 11:</b> Accuracy and Working of EfficientNet Models [45].....	33
<b>Figure 12:</b> Architecture of EfficientNet with MBConv .....	34
<b>Figure 13:</b> SoftMax Activation Function.....	36
<b>Figure 14:</b> Adam Optimizer Algorithm [69].....	38
<b>Figure 15:</b> Transfer Learning Technique .....	39
<b>Figure 16:</b> Pipeline of Proposed Methodology .....	41
<b>Figure 17:</b> Randomly Images Selected from Spine X-rays.....	42
<b>Figure 18:</b> Confusion Matrix of EfficientNet without Augmentation .....	44
<b>Figure 19:</b> Learning Curves without Augmentation .....	45
<b>Figure 20:</b> Confusion Matrix of EfficientNet with Augmentation .....	45
<b>Figure 21:</b> Learning Curves with Augmentation .....	46

## List of Tables

<b>Table 1:</b> Literature Review and Comparison of Classification.....	27
<b>Table 2:</b> EfficientNet B4 training parameters .....	31
<b>Table 3:</b> EfficientNet Performance Results on Transfer Learning Datasets [45] .....	35
<b>Table 4:</b> Parameters Detail .....	40
<b>Table 5:</b> Overall Structure of experiment without Augmentation.....	44
<b>Table 6:</b> Overall Structure of experiment with Augmentation.....	45
<b>Table 7:</b> Class-wise Accuracy with and without Augmentation .....	47
<b>Table 8:</b> Comparison of AASCE 2019 (SMAPE and ACCURACY).....	47

## CHAPTER 1: INTRODUCTION

The spinal cord, which connects the entire body from head to hip and forms an important connection between various human body components, is the main component of the human body. The spinal cord, which measures 40–50 cm from head to body and has a diameter of 1–1.5 cm, plays a key part in various gestures and motions, such as up and down. On either side of the nerve roots, two rows that are joined develop. There are 31 pairs of these nerves, which are a little bit spaced out from one another. The spinal cord has a cylinder-shaped structure and is divided into four segments: cervical (C), thoracic (T), lumbar (L), and sacral (S) [1]. While common spine curvature disorders are Scoliosis, Kyphosis, and Lordosis. Scoliosis is further divided into two segments that are C-Shaped and S-Shaped. According to their name, it creates C and S pattern shape in the spine. S shape indicates that S deformity has two convex sides which makes the more severe condition of scoliosis. In further there are two types of C-Shaped, the first one is Dextro-scoliosis (Right Side Curve) and the other one is Levo-scoliosis (Left Side Curve). While S-shaped further classified minor and major curves [2]. Scoliosis is a 3-D spinal disease in which the vertebra of the spine shifts from the body's midline to the coronal plane, causing the vertebral body to move side to side and the spine to bend. This causes a curvature to appear on an x-ray image [3]. Thus, the spread of Adolescent Idiopathic Scoliosis varies widely, with about 2-3% of the adolescent population affected by this [4]. 2.2% of teenagers required therapy, which included orthotics and other medical procedures [5]. According to the research statistics[3, 6], girls are involved more than boys among adolescents. In recent years data is increasing in all regions of the world. For severe conditions of scoliosis surgical treatment is required, therefore patient's condition depends on the degree of spinal curvature. Orthopedic doctors [5, 7] manually doing to examine the curvature of the spine. In the end, the measurement result of doctors and others is different due to the lack of Cobb angle manually. If the disease is matured, then patients have may a few symptoms like back pain, bloated curvature of the spine, shoulder pain, and unbalance alignment of the hip [8]. The World Health Organization (WHO) found that between 250K and 500K persons suffer from spinal damage due to various incidents, including car accidents, slips, falls, crashes, and other forms of violence [9]. These all issues can be addressed with the visualization of x-rays techniques. With the help of scoliosis classification, it will diagnose the curvature of the spine. It will facilitate the clinical specialist to determine the treatment of scoliosis which is performed on the patient. By using this technique, we may raise ConvNet's baseline to support any

resource while retaining model performance. The use of train and test time augmentation (TTA) tends to improve the performance of the model. There were augmented techniques employed, such as CLAHE, random flip, random brightness, blurring, cropping, and jittering.

## **1.1 Motivation**

Between 2% to 3% of people worldwide are affected by scoliosis. That might seem small, yet it is quite enormous. When we learn that between 140,000,000 and 210,000,000 people are affected, we recognize that scoliosis is not something that can be treated easily [10]. Most individuals are mindful of it but don't appear to get it, that's why we are here. Magnetic Resonance Imaging (MRI) made a significant impact to understand scoliotic deformity but is still evolving. Doctors use medical protocols to ensure the corrective shape of scoliosis. However, there is a chance of human error that may cause severe complications. To better detect detection systems, and diagnostic tools and developed a pre-trained model. The main target is to detect and classify scoliosis disease and it helps to prevent timely diagnosis and tells the spinal shape. It can facilitate in a very short time and is the motivation behind this research.

## **1.2 Problem Statement**

Precisely and opportune determination of Scoliosis illness has much noteworthiness in its treatment. Different imaging methods are used for this purpose but all in vain. Manual diagnosing with x-rays images is time-consuming and it may affect the bad results. Therefore, the purpose of this research is to facilitate the medical experts by providing an automatic service system to diagnose and classify scoliosis disease using spine X-ray images.

## **1.3 Aims and Objectives**

The following are the research's main goals:

- To use a pre-trained EfficientNet model to achieve higher accuracy
- Deep learning-based classification of scoliosis from x-ray imaging
- To detection of Scoliosis disease (S-shaped, C-shaped, Normal).
- Comparing before augmentation and after augmentation for more generalization.

## 1.4 Structure of Thesis

The structure of this work is as follows:

**Chapter 2:** The significance of scoliosis in human anatomy is discussed. It goes on to examine their varieties and signs

**Chapter 3:** An overview of the literature and key research for the diagnosis of scoliosis in recent years is provided

**Chapter 4:** The methodology including augmentation procedures and the classification of scoliosis were proposed

**Chapter 5:** All the results of experiments are described in detail with their figure and tables also introduce the dataset used for the performance evaluation

**Chapter 6:** Described the conclusion, contribution of research, and future scope



## **CHAPTER 2: SPINE CURVATURE AND ITS DISEASES**

The spinal cord is made of muscles, bones, tendons, and other tissues that extend from the base of the skull close to the spinal cord. Different types of spine curvature disorders are existing. The natural curvature of spines is rumped or exaggerated in some areas as occurs with some diseases, i.e., lordosis, kyphosis, and scoliosis. This chapter will briefly cover spine curvature diseases and their different types in detail.

### **2.1 Anatomy of Spine**

The spinal column provides the basic back of the entire body, allowing one to stand up, bend, and twist. The spinal column is a crucial component of the human body that carries out several functions, including correcting and developing. It enables upright posture, spinal column security, and shock absorption. Unique parts of the vertebrae and spinal column ensure that the spinal cord can communicate with the brain. Through the interplay of the bones, these elements cause disturbance throughout the body.

The spine is made up of 33 independently joined vertebrae, or bones, that are separated into five sections. the lumbar, sacral, sacral-lumbar, cervical, and coccyx spine bones. The cervical region of the spine is made up of seven vertebrae, from C1 to C7, that is joined to the skull's bony foundation. The atlas and axis, two of the best bones, are also mentioned. Cervical bones can perform the routine functions of the neck. The thoracic segment is located between the cervical and lumbar vertebrae at the level of the chest. This region of the spine is made up of 12 vertebrae, numbered T1 through T12, which connect to the rib cage. The lumbar region, which is made up of the five lumbar vertebrae L1 to L5, is located between the thoracic and sacral vertebrae. It could be a portion of the spine that supports weight. At the base of the spine, in the sacrum, there are no plates that separate the vertebrae. It features five merged levels, numbered S1 to S5. Additionally connected to the spinal column in this region is the pelvis. While the coccyx, which is made up of four fused vertebrae, also serves as the base of the spinal column.

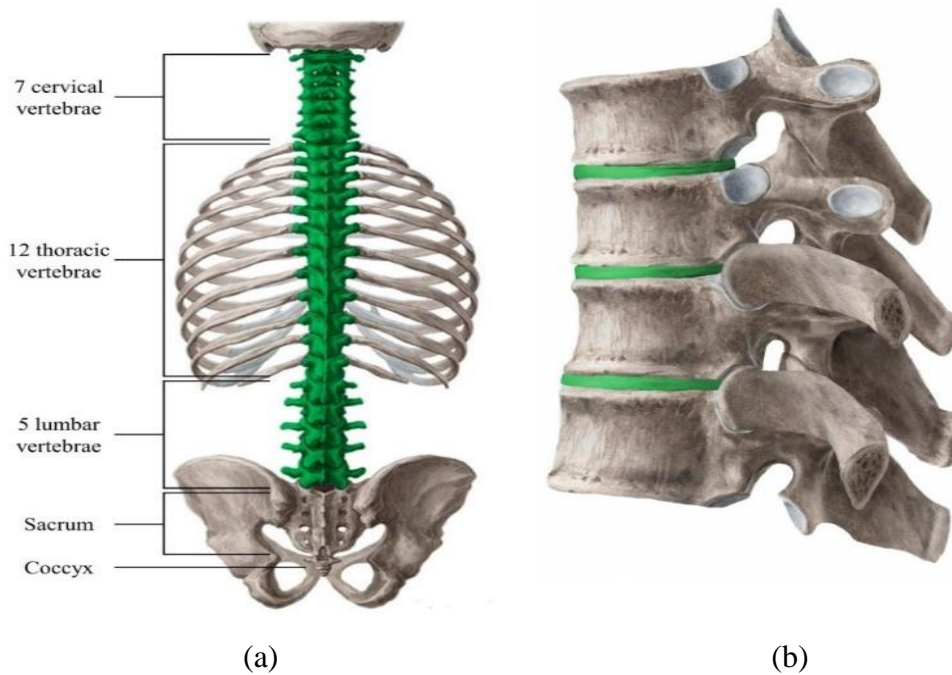


**Figure 1: Anatomy of Spine [11]**

(a) green highlighted indicates the part of the spine that contains individual vertebrae (b) Ligaments

### 2.1.1 Cervical Spine

Seven vertebrae (C1-C7) and six intervertebral plates make up the cervical region, which amplifies from the cranium to the base of the trunk, where the thoracic rib cage begins as appeared in Figure 1. The major function of the cervical spine is supporting the load of the neck and head while allowing rotation and protecting the spinal cord extending to the brain [11].

### 2.1.2 Thoracic Spine

The thoracic spine is the part of the spinal column which consists of 12 bones (T1-T12) [12]. It grows from the top of the lumbar spine and the bottom of the cervical spine. It controls overwhelming stack bearing and assurance of the spinal line, gives soundness all through the trunk, and interfaces with the rib cage which ensures the imperative organs such as the heart and lungs.

### **2.1.3 Lumbar Spine**

The lumbar spine comprises the lower conclusion of the spinal column between the thoracic spine and sacral spine (L1-L5). It permits the scattering of the axial forces. The spinal line runs through the center of the vertebral column and ends the conus medullaris at (L1-L2) [13].

### **2.1.4 Sacrum**

The concave sphenoid bone known as the sacrum is located near the base of the spinal column. It is an altered triangle, the base is found at the best, and the conclusion is at the bottom [14]. The sacrum comprises five vertebrae (S1–S5) which are associated with the pelvis at the sacroiliac joint and act like it were a skeleton interfacing between the trunk and the bottom of the body.

### **2.1.5 Coccyx**

At the base of the spine and beneath the sacrum, there may be a triangle-shaped channel of bone. It speaks to the vestigial tail but the common term is tailbone [15]. The coccyx's major functions including acts as an attachment for pelvic tendons, ligaments, and muscles. It is providing support and stabilizes the whole body while in a sitting position.

## **2.2 Intervertebral Discs**

The interverbal discs (IVD) play an important role in the functioning of the spine. It is the buffer of fibrocartilage and the principal joint between two spinal columns. The human spine has 23 discs, of which 6 are in the cervical spine (the neck), 12 in the thoracic spine (the center), and 5 in the lumbar spine (lower). It allows the spine to flex without a deal of great strength. It also provides a shock-absorbing effect and prevents the vertebrae from grinding to one another. It consists of three major types.

- **Nucleus Pulposus (NP)**

It is a gel-like structure which is consists of a center of Interverbal discs and provides flexibility to the spine with a great deal. It is made of 66% to 86% of water which consists of collagen and proteoglycans.

- **Annulus Fibrosus (AF)**

It comprises 15-25 layers of fiber bundles which are intense circular outside of an intervertebral disc that encompasses the internal core of the nucleus pulposus.

- **Vertebral Endplate (VE)**

It is the upper and lower endplate (0.5 -1 mm thick) that covers the inferior and superior aspects of the disc. It provides the main source of nutrition for the disc. The hyaline disc is the endplate of a disc to compromise the severe disc generation

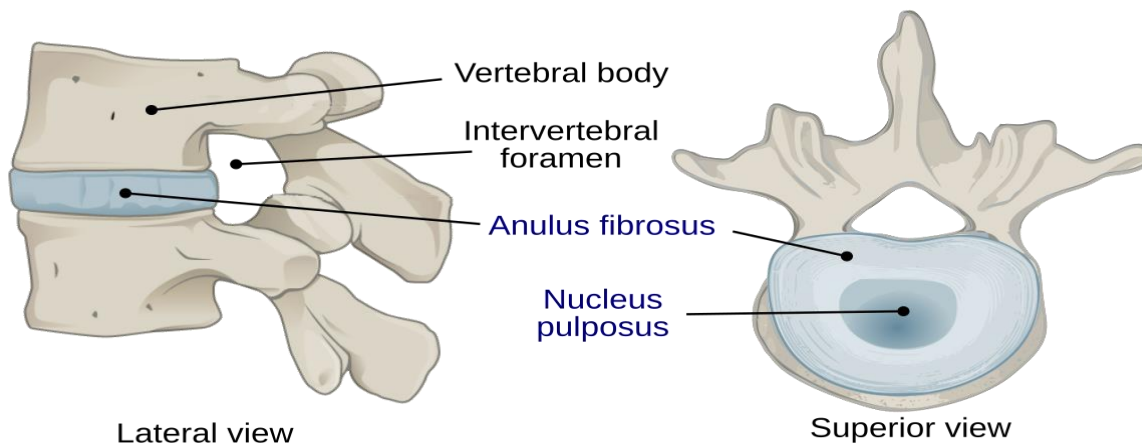


**Figure 2:** Intervertebral Discs

## 2.3 What is Scoliosis and its types?

Scoliosis is a spine curvature that is diagnosed in adults and children. Scoliosis occurs as the condition of cerebral palsy and muscular dystrophy. Some curvature worsens as children develop and some scoliosis can be debilitating. The spinal curve is the condition that diminishes the sum of space inside the chest, and it makes it an issue for the lungs to operate legitimately. A few individuals have mellow scoliosis which can be monitored closely with the assistance of x-rays to see the bends. In a few cases, there's no require for medicines and wear bracing to halt the bend from bracing. A few conditions require surgery to rectify the serious bends.

### 2.3.1 Different types of Scoliosis

There are four types of Scoliosis which are mentioned below.

- **Congenital Scoliosis (CS)**

It is the spinal deformity that is already present in the birth of people. In some cases, there is a bone malformation that can cause scoliosis. Incorrect bone formation causes the spinal curve. Medical experts are still confused about why people are born with bone malformation.

- **Neuromuscular Scoliosis (NS)**

The condition known as neuromuscular scoliosis affects children and impairs the body's ability to govern the muscles and support the spine.

- **Idiopathic Adolescent Scoliosis (IAS)**

Idiopathic Adolescent Scoliosis is most common in females. The average age of diagnosis is between 10 to 18. IAS also developed in infants, juveniles, and adolescents as well.

- **Adult De Novo Scoliosis (ADS)**

It's the fourth condition of scoliosis. Adults who have no history of scoliosis developed the condition fall which is 'de novo scoliosis. Spinal deformities occur because of degenerative changes of the spine that accompany aging.

## **2.4 Different Shapes of Scoliosis**

There are some curves which are describing types of scoliosis. S and C shapes described the curve's presentation. Their classification is separate from each other but linked.

### **2.4.1 Normal Curve**

The typical bends happen at the cervical plan to the thoracic plane which is named as "sagittal plan". Natural bends situated the head over the pelvis and worked as a stunning defense against stretch amid distinctive developments.

- **Coronal Plane**

The vertical plane that runs parallel to the shoulders and is coordinated from head to foot is what divides the body into its front and back halves.

- **Sagittal Plane**

Divides the body in half, left and right.

- **Axial Plane**

It is the parallel plane that connects the right coronal and sagittal plane points at the ground plane.

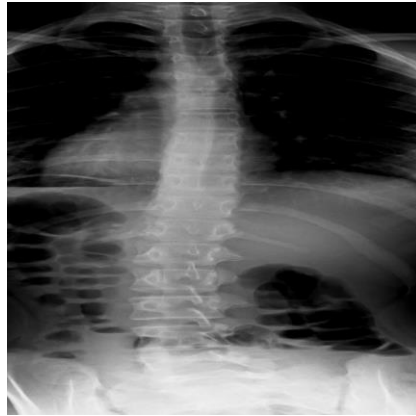


**Figure 3:** Normal Curve

### 2.4.2 S-Shaped Curve

S-shaped is also called a double scoliotic curve. In this curve the spine bend in different positions such as the lumbar and thoracic segments of the spine. An S-shaped curve has two parts, one part is the upper part, and the other is the lower part and both the parts bend in opposite directions. The upper part of the spine involved the thoracic spine (upper, mid), while the lower part involves the lumbar spine (low back). Then it will become two segments which are named the thoracolumbar curve and the cervicothoracic curve. The cervicothoracic curve occurs in the upper part of scoliosis and impacts the neck (cervical) as well as upper and lower back, while the thoracolumbar curve appears in the lower part of scoliosis which is mid-back (thoracic) and lower back (lumbar).

- **Symptoms**

- Smallest deviation of the head
- Asymmetry ribs
- Different alignments in the horizontal position of the waistline
- Increase the one-shoulder girdle
- Appear pain in the back, chest, and lower limbs



**Figure 4:** S-Shaped Curve

### 2.4.3 C-Shaped Curve

There are two types of C-shaped Scoliosis. One is Dextroscoliosis and the other one is Levoscoliosis. Dextroscoliosis occur when the spinal curve is on the proper side (right) while Levoscoliosis occur on the clear outside (left) of the spine. So, these two segments are called the term C-shaped scoliosis. It can be visualized when viewing the person from the rear.

- **Symptoms**
  - Inappropriate location of heading center
  - Lower back pain
  - Hip and shoulders appear uneven
  - One shoulder higher than the other

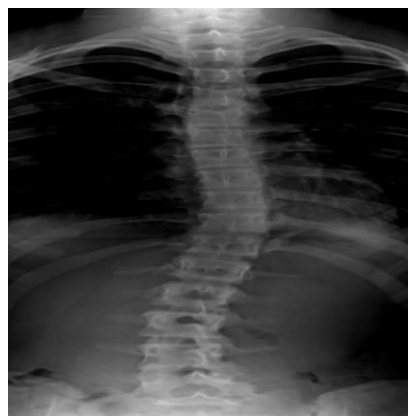


**Figure 5:** C-Shaped Curve

#### 2.4.4 Causes

Medical experts don't know about the causes of scoliosis because it appears due to hereditary factors while some disorders run families. Some important causes are mentioned below.

- Neuromuscular condition
- During the birth time, the development of bone of the spine
- Different injuries to the spine
- Spinal abnormalities
- Surgery effects on chest wall as a child

#### 2.4.4 Risks Factors

- Different symptoms and signs have occurred in adult
- In males and females, there is some sort of scoliosis developed at the same rate
- Scoliosis can also be developed due to family, but some children with scoliosis do have no disease in their family history

#### 2.4.5 Complications

Some people have not at any serious attack of scoliosis, it may have different causes and complications including:

- **Breathing Effects**

Within the extreme condition of scoliosis, the rib cage may be squeezed against the lungs and make it more troublesome to breathe.

- **Backache problems**

A few individuals who had scoliosis in childhood may be more likely to have serious torment than grown-ups. It happens when the spinal bend gets to be huge or is treated unevenly.

#### **Physical Appearance**

Scoliosis causes many noticeable distinctions, like an imbalance of shoulders, uneven hips, prominent ribs, and the shape of the human becomes a curve.



## **2.5 Methods and Technologies used for diagnosing the Scoliosis**

Medical imaging procedures are emphatically related to medical informatics. Each field of medicine is combined with distinctive advances in a computer science field, and it provides accurate results which are very helpful for the judgment of different diseases in a very short period. Physicians have hands-on experience with the software application and know how to utilize it appropriately. As a result, the medical field becomes an integrative science. Most applications meet the desires of the medical industry. Different techniques are used for diagnosing scoliosis some are mentioned below.

### **2.5.1 Method and Technique for Assessment of Scoliosis using radiography**

X-ray images are a frequent name for radiography. It is essential for imaging the spine and provides the projections: posterior-anterior (PA), anterior-posterior (AP), and lateral (LAT) [16]. X-rays take an image with 2D space images while scoliosis is in 3D condition. As a result, an x-ray combined the measurement and provide a comprehensive understanding of the condition. However, it is a very gold standard method to diagnose scoliosis as compared to others because other methods are too indirect and expensive.

### **2.5.2 Method and Technique for Assessment of Scoliosis using Magnetic Resonance Imaging (MRI)**

Magnetic Resonance Images (MRI) are a non-intrusive strategy to discover increasing applications for the improvement of specialized strategies and arrangements [16]. It has a magnetic moment with an advanced computer service system and radio waves. As a result, it produces detail of the part of the body without the use of radiation.

### **2.5.3 Computer Tomography (CT)**

Computer tomography uses computers or x-rays computers to create a cross-section view of the body. It allows the physician to see the inside of the body at different levels. CT scans can be used for every part of the body. It produces images in slice form and is easily visible.

### **2.5.4 Ultrasound**

Applying ultrasound [17] to look at the body's interior structure to verify the scoliosis assessment. It is the image of every part of the body shown on the computer screen.

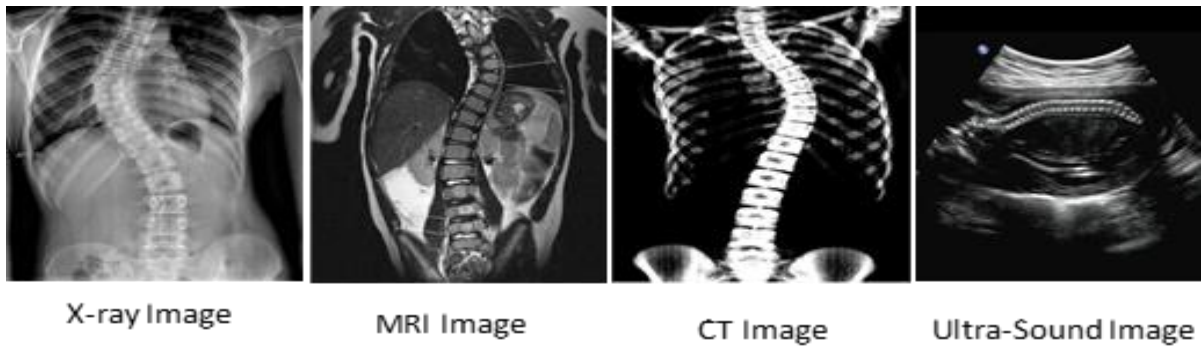


**Figure 6:** Methods for Analyzing Scoliosis

## 2.6 Treatment of Scoliosis

Treatment of the spinal bend depends on the seriousness bend. A few children who have may mellow bends ordinarily don't require any treatment. Although they may get to ceaselessly checkups for the seriousness of the bend as they develop. Bracing and surgery are important in the treatment of the severe condition of the curve. Some factors are including:

- The growth of bones has stopped in children then the severity of the curve will be low, which means the braces have an imperative calculate in children whose bones are still developing
- Bones severity can be checked with X-rays
- Girls have more curve growing probability than the boys

### 2.6.1 Braces

If a child's bones grow rapidly then it has moderate scoliosis, then medical experts recommend braces. With the help of braces, it won't remedy scoliosis or switch the bend but it as a rule avoids the bend from getting more awful. The objective of bracing is to the advancement of restorative appearance and to preserve the by and large body arrangement and adjust amid development [18]. A common type of brace is worn under the clothes, and it is not visible most braces are worn 13 to 16 hours a day. Braces are suspended when there are no changes happened within the height. Young ladies completed age development at 12 and boys at 16 but it shifts by person.

## **2.6.2 Surgery**

Surgery can ordinarily be done, when the bend is more noteworthy than 40 degrees [19]. However, if anybody has been diagnosed with scoliosis and feels the curvature inside the body which causes discomfort, then surgery is the best process to take it in position. Spinal fusion could be a standard handle for surgery. Medical expert fuses vertebrae using rods and screws. Rods aid keep the spine straight and screw hold it in right put. Inevitably, the bone joins, and vertebrae meld into a single bone. This bone joint comprises bone materials. Whereas in children bars can be balanced as they develop. A few of the dangers are taken amid spinal fusion surgery.

- Bleeding
- Backache
- Infection
- Nerves damage

## **2.7 Exercises for Scoliosis**

Exercise is the conservative method for scoliosis patients. Besides routinely used exercise for scoliosis which is mentioned below.

### **2.7.1 Individual therapy of Scoliosis**

Numerous components were chosen from the treatment of scoliosis that has been adjusted from distinctive concepts of treatment. This treatment was concocted in Poland, for the good thing of postural issues and scoliosis. This method is used for the therapy of idiopathic scoliosis and supportive therapy is used for bracing and preparation for surgery. It may be used after surgery for the alignment of shoulders and pelvic girdles [20].

### **2.7.2 Spine Core method**

This method consists of a combination of accurate movements and muscle rebalance exercises [21].

### **2.7.3 Lyon approach**

This method is used for physical therapy, and which consists of a combination of Lyon braces. In this approach, three parameters are considered with it, including Cobb angle, postural imbalance, and patient age [22].

### **2.7.3 Dobomed physical therapy**

This strategy was too designed in Poland which tells us about trunk distortion as well as respiratory work impedance. This strategy has required high power of patient cooperation. Be that as it may, it isn't appropriate for children [22].

### **2.7.4 Barcelona physical therapy**

It is a physical treatment strategy that can organize the treatment plane of cognitive kinesthetic preparation and sensory-motor as well. This treatment works on the suspicion that scoliosis poses and imbalance of delicate tissues promote curvature progression [23].

### **2.7.5 Scientific exercise for scoliosis**

This method is organized from scientific principles it is an expansion of Lyon's approach. It comprises four diverse standards, making strides in the mindfulness of understanding deformation, independent rectification by the patients, utilization of exercise to invigorate the adjusted response, and utilization of brace scoliosis-specific exercise [24].

### **2.7.6 Schroth method**

Katrina Schroth developed this plan in Germany in 1927. Scoliosis must be corrected in three measurements in this case. This strategy points to decreasing scoliosis development, decreasing postural turn, and aiding preserve mobility, and postural stability. It also helps to the reduction of pain and improves cardiopulmonary function in scoliosis [25].

## **2.8 Other diseases of Spinal Deformity**

### **2.8.1 Kyphosis**

It is a type of spinal deformation in which spine bends happen within the outward position and create the problem of the hunchback, called hyper kyphosis.

- **Chin on chest syndrome**
- Head dips and head ptosis are evident, and the cervical and top thoracic regions are both very significant.
- **Symptoms**
  - Shoulder round
  - Fatigue
  - Weakness
  - Spine stiffness
  - Hump on back
  - Breathing difficulties

## 2.8.2 Lordosis

It is also a spinal deformity in which the spine curve occurred at the inward position, called hyper lordosis. It differentiates the normal spine from the lumbar spine.

- **Symptoms**
  - Pain in spine
  - Metabolic disease
  - Violation of normal curvature spine
  - Stretches of muscles
  - Compression of internal organs
  - Impaired posture
- **Flatback Syndrome**

It is the spinal deformity that occurs when the lumbar spine loses its normal lordosis.

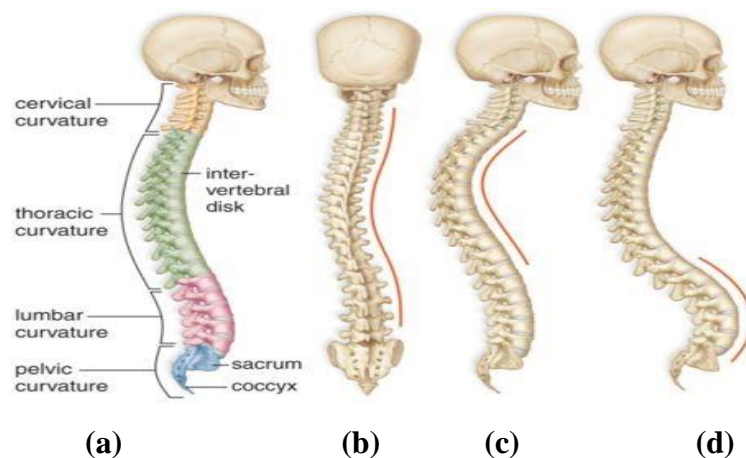


**Figure 7:** Comparison of Scoliosis, Kyphosis, and Lordosis

(a) Normal (b) Scoliosis (c) Kyphosis (d) Lordosis

**In chapter 2**, we have discussed the background knowledge, and different techniques to classify scoliosis disease. First, described the overall anatomy is shown in figure 1. There are different vertebrae presented in the spinal cord and discussed one by one in detail. Intervertebral discs play a vital part in the working of the spine which comprises 23 spine columns. All their types are also described in detail. While scoliosis is the disease of the spine and fully discussed type with its different shapes and curves as well which are shown in their figures. To validate the scoliosis condition, additional techniques such as computer tomography (CT), magnetic resonance imaging (MRI), radiography, and ultrasound are also used. According to these assumptions. Radiography performed excellent results to verify the correct disease of scoliosis. different techniques used with the different testing processes by helping their machines. We discussed how to overcome scoliosis diseases with different exercise techniques and surgical operations.

Moreover, we have also discussed the causes, symptoms, and risk factors associated with scoliosis. Some of these risk factors affect breathing, backache, and physical appearance problem which are already discussed in this chapter. Some medical experts did not know about the real fact of scoliosis because it appears due to hereditary factors while some disorders run in their own families. All these issues are discussed in this chapter in detail with their different types and figures.

## CHAPTER 3: LITERATURE REVIEW

Radiographs have always been an area of interest for researchers in medical imaging. Although various imaging techniques are now being utilized. X-ray images are utilized to identify spine deformities in human anatomy. In the last few years, researchers made a lot of potentials and published state-of-the-art Computer-aided Detection (CSD) models to detect and classify different types of scoliosis disease using AI algorithms. Among those, few are solely focused on effective segmentation and others have also developed classification techniques for disease diagnosis. This chapter will summarize and compare all the research in the domain of medicine for the detection of scoliosis disease using deep learning. The determination of spinal clutters and other variations from the norm inpatient can moreover be done physically through side effects. But due to the advanced techniques, the most authentic method for diagnosing the spine are X-ray images.

### 3.1 Data Augmentation

Inoue, H. et al. [26] proposed fresh training using image classification techniques for data augmentation. Remove some of the noisy data from the dataset. By putting another data image, they chose from the training data on top, they applied new patterns from the data image. Make  $N^2$  samples of  $N$  samples in the training data by picking images at random from the training set. All the evaluated dataset's classification accuracy was greatly increased by this method. They described several datasets where the top 1 mistake was decreased, from 33-5% in the ILSVRC 2012 dataset to 29%, and similarly in GoogleNet from 8.22% to 6.93% for the CIFAR-10 dataset. They demonstrate how this method is particularly beneficial for achieving high accuracy on very tiny datasets. For categorizing medical data, this method is more useful. Perez, L et al. [27] explore the multiple problems of data augmentation to classify the images. They accessed the small subset data of ImageNet data and compare all techniques of data augmentation. The most successive technique is traditional transformation. They also used GANs for the generation of images with different styles. In the end, they propped the method of a neural net to apply the augmentation technique to improve the classification, which is called neural augmentation.

Ma, B., et al. [28] organized a novel-based strategy to address the insufficient amount of data. in this strategy, they realize the fusion of real data and augmentation techniques used for the mining process. For the grain occurrence image segmentation, they hereditary manufactured

information by interfacing the image which is chosen from the fortified physical instrument of grain arrangement and image style from the original data. the results show that only 35% of data achieved segmentation performance from a trained model of original data. because the time is necessary for the grain formation and generate synthetic data as well, are almost neglected as comparatively data obtained from the original. They suggested using deep learning techniques in this research without increasing the amount of training data.

Aggarwal, s. L. P. et al. [29] aim of this paper to recognize the different diseases by using data augmentation, such as acne, rosacea, psoriasis, impetigo, and atopic dermatitis. For this, they gathered the data from dermatological images by using retrain TensorFlow inception version 3. they performed once with and without once data augmentation and R software was used. As a result, adopting data augmentation boosted statistical analysis. The Mathew connection coefficient grew by 7.7% after that. Each disease boosted the area under the curve (AUC) of the region by employing data augmentation, with an average increase of 0.132 and a standard deviation of 0.033. The greatest AUC was 0.18 for atopic dermatitis, while the lowest AUC was 0.87 for psoriasis when employing data augmentation. The best AUC was 0.97 for acne.

Fawzi, A., et al. [30] data augmentation used for the transformation of training data and creating new samples. The purpose of this paper is to automate adaptive algorithms for selecting transformation samples by using data augmentation. After that process, they integrate the data augmentation into Stochastic Gradient Descent algorithms to train neural networks. They performed on the two datasets and the proposed scheme performs well for random data augmentation concerning accuracy and robustness.

Tran, T., et al. [31] although it is a very powerful technique for a generative demonstration for constructing new training samples, fresh training samples are derived from the data augmentation. They worked on the unique Bayesian formulation for this paper. The distribution created by training is then produced by new annotated points acting as lost variables. introduced the generative adversarial network extension algorithm known as generalized Monte Carlo expectation maximization (GAN). They achieved significantly improved results on MNIST, CIFAR-10, and CIFAR-100 after employing this method.

Shijie, J., et al. [32] proposed different methods of data augmentation for image classification on an image classifier by utilizing a deep CNN model. In this paper, they selected Alexnet, because they used already the pre-training network and variants of CIFAR-10 and ImageNet as a real dataset. Data augmentation techniques used include GAN/WGAN, shifting, cropping, color jittering, noise, and a few other combinations. As a result, it shows that four methods



perform better as compared to the other combinations such as Rotation, flipping, cropping, and WGAN, while some methods are more effective in work than in individuals.

Mikołajczyk, A. et al. [33] examined and evaluated data augmentation methods used for the image classification challenge. They presented their research on data expansion approaches like data augmentation for their work on imaging style transfer. It produced a high-resolution image that appears to be another image while being the base image. For that training model, recently developed photos are used to advance the preparation for handling effectively. The three types of medical cases—skin melanomas determination, histological images, and breast magnetic resonance imaging—all make use of the proposed technique. used a classification method to diagnose these classes.

Zheng, Q., et al. [34] developed a comprehensive framework for enhancing data that makes use of the deep convolution neural networks (CNN) model to improve accuracy. It plays a significant role in implicitly creating model ensembles without incurring additional training expenditures. The capacity to generalize was improved by data augmentation, which can also guarantee network optimization during the training and testing phases. The challenge of providing reliable information about a particular area is data augmentation. Any deep learning problem can be coupled to this framework because it is universal. Only the CIFAR-100 fine-grained dataset (70.22%) and CIFAR-10 coarse-grained dataset (93.41%) can be classified as images based on the peak test findings. It illustrates how well the framework works.

Wickramanayake, S., et al. [35] proposed a methodology that is based on the previous work that used concept base explanation to augment the dataset into new images to represent the region for improvement of the model performance. This method is also able to explain generated classifiers and post-doc interpretable from the black-box classifier. The proposed technique comes about to appears as an approach in many ways better concerning classification as related to the other state-of-the-art methodologies.

Gu, S., et al. [36] the work they did to improve image classification was presented. They expanded both the data and the neural networks for this using the data augmentation technique. To minimize within-class disparities and retain sensitivity to between-class variation, they employed the CIFAR-10 dataset. With this approach, the loss function is minimized while yet achieving improved accuracy. The different architectures are used to avoid overfitting which is monitored by the data augmentation and hyperparameters. To evaluate the model performance, they used training and testing datasets with their accuracy and loss. For large-scale image classification, they used the VGG16 model. After applying this model, achieved a training accuracy is 96% and a testing accuracy is 92%. So, their work shows the overall error

rate dropped to 8%. Meanwhile presented workflow of model architecture, data augmentation and hyper-parameters are very useful for avoiding overfitting and help to produce better results for classification.

### **3.2 Classification**

S. K. Wardani et al. [5] used the classification procedure to work on the class scoliosis disease and used it in the image processing strategy. The preprocessing of spinal bone images included the use of a morphological watershed and median filter. The x-ray images were then classified using an artificial neural network technique, with a success rate of 99.74% and an error rate of 0.26% for segmenting the spine.

R. H. Alharbi et al. [37] proposed automatic measuring of the Cobb angle using X-ray images while this dataset was collected from King Saud University (KSA) and the CLAHE method was used for the imaging process then Neural Network was applied for detection of vertebra in X-rays images. Then compare the results with experts' manual measurements and achieve 90% accuracy.

Obeid et al. [38] develop the classification of coronal spinopelvic malalignment. It is implemented on a retrospective review of coronal misalignment (CM) that identified distinct patterns. After the identification of each category, each pattern could be specified. were distinguished as possibly impacting surgical methodologies such as coronary curvature stiffness, mobility, and decaying of the lumbosacral junction. However, by combining different patterns and modifiers, surgical algorithms are proposed to manage each situation.

In [39, 40] used a regression model with a different combination of techniques. B. Khanal et al. [39] Faster-RCNN was used for the location of vertebrae while DenseNet was used for landmark regression. Six-order polynomial curves produce better results and boost the net for Cobb estimation. It produced SMAPE up to (25.69).

R. Tao et al. [40] ResNet50 used a combination with Feature Pyramid Network (FPN) to extract region suggestions and generated SMAPE in (25.47).

Z. He. Et al. [41] proposed automatic detection of representative features by using the Bilateral CNN method to classify NF1-S. This method is implemented on the AP and X-ray images as well. Moreover, other methods used spine deformity for auxiliary diagnosis. 87.92% accuracy was achieved with these techniques as compared to other techniques ranging from 52.58% to 83.25% with fivefold cross-validation.

N. Sabri et al. [42] X-rays are used to identify the type of spinal deformity. 2D photogrammetry was used to classify the types of Lenke's scoliosis. To categorize Lenke's type, a convolutional neural network (CNN) was utilized. Three convolution layers with a filter size of 3x3 produced more accuracy than other filters, according to experiments on 2D photogrammetric images. This shows that image size is important for best results and running an image input size of 180x180 yields high (84.6%) accuracy.

Z. Tan et al [43] purposed an automatic system that also obtained measuring methods of scoliosis by utilizing deep learning models to improve the accuracy using X-ray images. U-net segmentation is applied for image segmentation. The top, and bottom vertebrae, and slopes of the endplates were recognized by the least-squares and bounding-rectangle methods. The angle between the UEV upper endplate and the LEV lower endplate is referred to as the Cobb angle. Comparing the measured Cobb angle results with the calculated Cobb angle results, one can see similar results. This system assists doctors in clinical diagnosis.

S. Rothstock et al. [44] suggested machine learning methods categorize scoliosis patients according to asymmetry patterns on the surface of the trunk. With 50 patients, tests on Cobb angle and spine curve patterns were conducted. Every patient's trunk in the prior study had an uneven gap between their original and echoed torsos analyzed. The categorization of a patient's Cobb point and Augmented Lehnert-Schroth (ALS) classification, which is based on a torso asymmetry distance map, is done using an Associated Neural Organize. The results show a 90% accuracy of curve seriousness and a range of 50% to 72% among those with ALS.

Inspired by better performance of the scaling method and carefully balancing. M. Tan et al. [45] identify a new scaling model for all dimensions and works parallel using the compound coefficient, these dimensions are width, depth, and resolution as well. The effectiveness of this is to scale up MobileNets and ResNets. Further, they use neural architecture design for the new model and scale it up, which is Efficient-Nets. It performed better accuracy than previous models. EfficientNet-B7 achieves the highest accuracy on the data of Imagenet. 84.4% in the top 1 and 97.1% in the top 5 on ImageNet. EfficientNet-B7 is 8.4x smaller with fewer parameters and 6.1x fastest than the other models.

C. Vergari et al [46] proposed classification algorithms for automatic detection of scoliosis (brace, implant, no treatment) with help of posterior-anterior radiographs. By putting together, a forward convolutional neural network (FCNN) for analysis, a classification model was developed. Tenfold cross-validation was used for model validation. On radiograph images, the classification model had a 98.7% accuracy rate and a 2% misclassification rate. While 2.1% of reference group radiographs were incorrectly classified, the accuracy of brace radiograph

detection was 99.7%. Following the application of this method, 98.3% of the radiological pictures were accurately identified as brace, implant, or reference.

J. Yang et al. [47] developed a deep learning model-based approach for automated scoliosis detection on naked back images. The automatic localization of the region of interest detection using Faster-RCNN42. During the preprocessing stage, the images were sent into the Resnet, which collected high-level features for binary and multiclass classifications. Following this process, the performance was evaluated using the five-fold cross-validation technique, which produced a result of 0.94% for recognizing situations with a curve less than  $10^\circ$ .

X. Guo et al. [48] bolstered the scoliosis framework for a single curve. To accomplish the goal, they presented their work on an advanced recurrent neural network that is a long- and short-term memory network. Scoliosis is a classification and regression problem within this paradigm. They first created a network for classification before creating a model of the current degree of scoliosis that may be divided into three categories using objectively measurable variables like body height or arm span. The model's AUC for the mild, moderate, and severe classes was 0.90 percent, 0.94 percent, and 0.95 percent, respectively.

R. Korez et al. [49] proposed their work on the base of 3-D CT images. It worked on the automated detection and segmentation of the spine and vertebrae as well. Work depends on interpolation theory. The optimization technique was applied to the 3-D image, which is dependent on where the spine is, to pinpoint the exact placement of the entire spinal column. It is established where each vertebra is located. Following the discovery of vertebrae, the Dice coefficient in this phase was 83.6%.

Magnide, E., et al. [50] presented their research using EOS radiograph images to determine Risser sign maturity using machine learning methods. In this work, the pelvis left or right femoral heads, and left or right humeral heads are the areas of interest. They used a convolutional neural network of the ResNet101 type to work on 24 picture features that were retrieved from the radiograph images. Then, classify the Risser sign utilizing a support vector machine (SVM). The accuracy for iliac crests, humeral heads, and femoral heads was generally 84%, 78%, and 80%, respectively.

Li, J., et al. [51] supported the automatic scoliosis approach to the segmentation of the vertebral body and U-Net networks. From the segmented data, these algorithms automatically generate clinical assessments of coronal and sagittal deformities. While the mean is just under 0.33, the technique in this case showed an absolute normalized error of less than 0.35 in standard deviation. Their primary contribution is the provision of the clinical parameters for the personalization of spinal therapies and surgery.

Ha, A. Y., et al. [52] aim of validating the automatic approach to the cobb angle, and comparing the results of AI-generated and human reports generated in clinics. For this, they have datasets of 70% training data and 10% validation, and 20% testing images as well. Faster R-CNN ResNet101 was used for object model detection. The cobb angle parameters are determined by localizing the vertebral centroid coordinates using controller methods. AI-generated and human-generated reports are compared, and spearman rank order demonstration produced a correlation of (0.89,  $p < 0.001$ ). while the mean difference for both was  $7.34^\circ$  (95% CI:  $5.90-8.78^\circ$ ).

Tu, Y., et al. [53] DU-Net identification and segmentation have been proposed for the removal of unnecessary regions and segmentation of the spine contour in the spinal x-ray images. For scoliosis images, aggregate channel features for pedestrian detection algorithms were included to locate the spine area. The spine curve is adjusted into the spine contour since DU-Net served as a spine counter's trainer, and the spinal curve is then detected using a cobb angle measurement. Because of this, the detection system generated an average precision and recall of 98.5% and 99.5%, respectively. In contrast to IOU's 82.29% and DU-86.30% Net's precision, Dice's average coefficient for segmentation to reference is 90.28%.

Makhdoomi, N. A., et al. [54] worked on the diagnosing and treatment of scoliosis including spinal injection, braces, and different types of surgeries. Convolutional Neural Network (CNN) method and AI-based algorithms are used for detecting and classification of scoliosis disease. First, they preprocessed the dataset, then applied segmentation features, performance measurement, and then classification. For this, they used U-Net and achieve the results with an accuracy of 94.42%.

Fraiwan, M., et al. [55] proposed automated tools for the x-ray images. Scoliosis and spondylolisthesis were diagnosed using deep transfer learning. They gathered information from 338 X-ray images of three classes, including (188 scolioses, 79 spondylolisthesis, and 71 healthy). The three classes and the pair binary classification were structured using deep transfer learning models. Of the three courses, they scored the highest with 96.73% and 98.02%. The best accuracy of 98% was attained for the pair-wise binary classification.

Caesarendra, W., et al. [56] A deep learning architecture has been created to forecast the cobb angle and identify spine vertebrae from x-ray images. The anterior-posterior X-ray image local images and dataset from the AASCE MICCAI 2019 were used for training and testing. A convolutional neural network is used to automatically calculate the cobb angle. The proposed methodology, which is superior to clinical assessment (intraclass correlation coefficient  $> 0.95$ ), estimates the cobb angle with an accuracy of up to 93.6%.

R. Hamzah et al. [57] aim for this work, medical experts, surgeons, and academicians face many problems regarding scoliosis and their types that resemble the spine normal. They proposed a method to speed up the work by using machine learning approaches to solve the issues. Using radiological images, the grey level Co-Occurrence Matrix (GLCM) linked with ensemble classification that is Ada boost is used to distinguish between the normal spine and scoliosis. Following the implementation of this procedure, they automatically attained an accuracy of 86.67%.

N. Sabri et al. [58] suggested a photogrammetric strategy to get around problems with radiographic images. Lenke type-1 or non-type-1 scoliosis was classified using a photogrammetric of the human back. Classification is done using convolutional neural networks, which have layers for convolution, pooling, softening, and fully connected layers. This method's main objective is to assess the Lenke system's categorization by contrasting the average and maximum pooling results. While max pooling had high accuracy (84.6%) compared to the norm.

A. A. Abdullah et al. [59] purpose of this paper was to identify the parameters of spine abnormalities which is based on the physical spine collected data. Both supervised and unsupervised learning was done using a variety of machine learning approaches, such as Random Forest (RF), K-Nearest Neighbors (KNN), and Principal Component Analysis (PCA). As a result, they compared the result of the RF and KNN classifier. KNN achieved better accuracy as compared to RF since the percentage of KNN is 85.32% and RF is 79.57%.

A. Ha, et al. [60] scoliosis x-rays of the human body were used to develop an automated method for determining several skeletal maturity groups. They first utilized some class region networks to extract the human head and pelvic region, which are based on the Oxford Bone Score. The next step was to parallelize each stage of the region by scaling the convolutional neural network using a variety of chemicals. They achieved an F1 score of 0.99%, an overall accuracy of 0.89%, and an intraclass correlation value of 0.84%.

GA. Lein et al. [61] aimed to examine the vertebrae column and vertebra and build a tangent on x-ray images using algorithms. They employed clinical practice algorithms as tools for automatically analyzing patients with scoliosis. For this, 300 digital x-ray photographs of children's spines were employed. The neural network is trained and validated using this dataset. After comparing the findings, they were able to calculate the Cobb angle with an accuracy of 85%.

V. Miglani et al. [62] ability to classify skin lesion which has seven different types. It worked on the deep neural network. They worked with the unique HAM10000 dataset, which

comprises 10015 dermatoscopic images divided into seven different groups. The purpose of this study is how EfficientNet models convert the skin classification experiments with ResNet architecture. After that, they found EfficientNet model performs well as compared with the ResNet with fewer parameters. They obtained high AUC and ROC for each classification category; the average AUC values for classification for macro and micro are 0.93 and 0.97, respectively, whereas the ResNet50 model obtained 0.91 and 0.86.

S. Wang et al. [63] An approach is proposed that directly inverts the Cobb angle from an x-ray image. To correctly divide the two spine boundaries, they initially proposed a segmentation network. They generated high-accuracy regression predictions for the Cobb angle by feeding the resulting border score map and the original spinal X-ray images into a second angle estimate network. Using data from the AASCE challenge, they attained a SMAPE of 22.1775.

P. Chen et al. [64] proposed the work on spinal surgery diagnosis standardization and automation. To categorize the images of the spine, they used FRCCN and ResNet. They obtained the dataset of x-ray images for this study from the radiology division. They evaluated the orthopedic surgeon's results, examined their measures, and ultimately suggested an evaluation based on their findings. For scoliosis diagnosis, their results meet the clinical needs which are without the manual investigation of the x-rays scan. The computational approach developed for their clinical department is useful for their needs.

M. Raihan-Al-Masud et al. [65] recommended using machine learning techniques to standardize and automate the process of detecting spine problems. They are utilized in the PCS pre-processing stage and the univariate feature section. For the anomalies of the spine, algorithms like SVM, logistic regression, and bagging SVM and bagging LR ensembles are applied. They applied these methods to the publicly available dataset of 310 patients who have involved spine abnormalities. After applying these models to the training dataset, they have achieved the accuracy of all models are 86.30%, 85.47%, 86.72%, and 85.06% respectively. While applying these models to the test dataset, they achieved an accuracy of are same of 86.96%. However according to their experiments and results bagging SVM is more efficient, because compared to other models, it has a higher recall value and a lower missing rate. So, they used this model for the classification of who has been involved in spine abnormalities.

F. Galbusera et al. [66] analyzed the machine learning techniques essential for the accomplishment of tasks including speech recognition, natural language processing, and computer vision. They examined strategies that are particularly useful for spine research in this and offered a unique methodology based on them. Additionally, they briefly discussed the spine-related issues with machine learning and artificial intelligence in their work, which was

published quite quickly. The potential of biased judgments, data privacy and security difficulties, and finally the main concerns about AI in healthcare were discussed.

A. Amin et al. [67] presented a computer-aided approach to the detection and classification of scoliosis. Scoliosis is diagnosed through X-ray imaging. For this, they used EfficientNet-B7, the foundation of CNN, and deep learning techniques to deliver a rapid and faster response to scoliosis disorders like S, C, and Normal shaped. In the first step, they classified the scoliosis curves on the spine x-ray images using the EfficientNet model without any additional data, and they got an accuracy of 78%. The same model was used to categorize the curves in the subsequent stage, but this time they improved the data using the data augmentation technique, which resulted in an accuracy of 86%.

W. Caesarendra et al. [68] proposed the deep learning architecture for the detection of the spine using the publicly accessible dataset of AASCE 2019. The training and testing were done with a convolution neural network. From the spine x-rays, seventeen vertebrae were found, yielding 68 landmark features. These characteristics were then processed to calculate the Cobb angle and determine whether scoliosis was present. They further categorized the classifications into mild, moderate, and severe, and they achieved an accuracy of almost 0.9 (90%).

**Table 1:** Literature Review and Comparison of Classification

Year	Author	Techniques	Database	Accuracy (ACC) (%)
2018	S. K. Wardani et al. [5]	Artificial Neural Network	Surabaya Haji Hospital.	99.74%
2020	R. H. Alharbi et al. [37]	CLAHE. CNN	King Saud University (KSA)	90%
2021	Z. He. Et al. [41]	CNN, VGG-16, ResNet-50	Local	87.92%
2019	N. Sabri et al. [42]	CNN	Local (Lenke type)	84.6%
2018	Z. Tan et al [43]	U-Net segmentation, Scoliosis detection using Cobb angle measurement	Shenzhen University General Hospital	96%
2020	S. Rothstock et al. [44]	Fully CNN used to classify Cobb angle measurement, ALS	Local Dataset of 50 patients	75%
2018	J. Yang et al. [47]	Faster-RCNN42	Local Dataset of School Students	94%
2021	Magnide, E., et al. [50]	ResNet101 type convolutional neural network, SVM	Dataset of the femoral head, humeral head, and iliac crest	84%, 78%, and 80% respectively for three classes
2022	Makhdoomi, N. A., et al. [54]	CNN, U-Net	Dataset of children between 10 to 12 (Local)	94.42%.
2022	Caesarendra, W., et al. [56]	CNN	AASCE MICCAI 2019	93.6%
2018	A. A. Abdullah et al. [59]	PCA, KNN, RF	310 patients (Kaggle)	KNN 85.32% RF 79.57%.



## Research Gap

Researchers have already worked on the automatic detection and classification of scoliosis from spine x-rays images. A lot of the researchers worked on trained deep learning models to detect and classification of scoliosis. They often used CNNs, ResNets, U-Net, and other existing techniques in their model. In our experiment, we used EfficinetNet B4 for training and it is the family model which ranges from B0 to B7. It is a special technique for classification and computer vision tasks as well. While the researcher used ConvNets, at some point, the depth of CNN scaled up and create vanishing gradient issues, which cause the effect of low performance. After that researcher also used Resnets, to overcome the problem of CNN, ResNet was used for the skipping connections, but it is also required for manually fine-tuning. However, in our case, we used EfficinetNet for classification work which provides better accuracy than other models. On the AASCE 2019 dataset of 609 x-ray images, which comprises a multiclass problem, we trained our model. Due to the small dataset, to improve the dataset and applied the model, we used data augmentation techniques. Compound scaling, which identifies that scaling dimensions are not independent, is another primary justification for utilizing the EfficinetNet. Increase the network depth and balance the dimension for high-resolution images to obtain an accurate ratio. We used the transfer learning approach which plays an important role to become the model faster in the training process and make it generalized and easy to debug.

## CHAPTER 4: PROPOSED METHODOLOGY

The goal of this study is to demonstrate automatic scoliosis detection and classification from spine x-rays using transfer learning and EfficientNet. Our proposed work consists of scoliosis which has three types (Normal, C-Shaped, and S-Shaped) and classified these types. We have used Efficient-Net B4 for the classification of these types using the augmentation technique.

### 4.1 Classification

Transfer learning, based on the convolutional neural network utilizing the EfficientNet model with pre-trained weights on ImageNet, is used to automatically detect and classify scoliosis from x-ray images. EfficientNet is dependent on several models ranging between B0 and B7. The model may preprocess the input and produce precise output when used for feature extraction. The parameters are then minimized to prevent overfitting using Global Average Pooling. In this, the three-dimensional tensor's spatial dimensions are condensed using Max-pooling layers. SoftMax is used to classify each class with the assigning of probability, while the sum of this probability ranges from 0 to 1. The abstract level diagram of our framework is shown in figure 8.

To train, we used AASCE 2019 dataset x-ray images divided into three classes: normal, C-shaped, and S-shaped. Between training and validation, we divided the data 80:20.

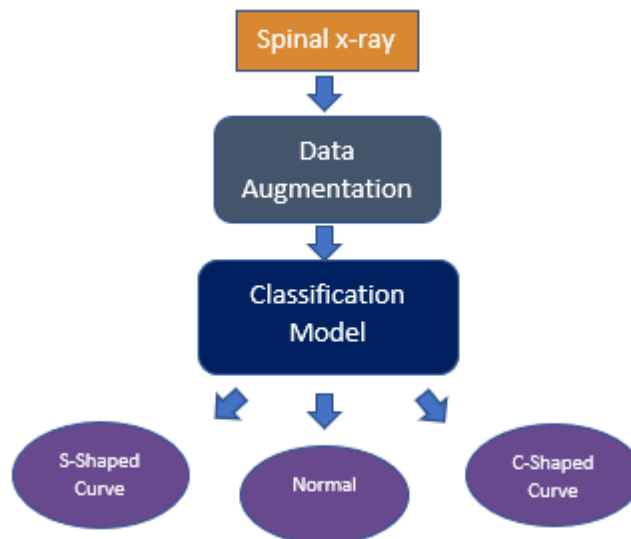


**Figure 8:** Abstract Level Diagram of Classification

## 4.2 Data Augmentation

Augmentation is an essential phenomenon of training discriminative Convolution Neural Networks (CNN). It arranged many tactics, including random cropping, horizontal flips, and Principal Component Analysis (PCA), which highlights the traits of the original images. Data augmentation is commonly used in medical images for classification especially. It is referred to as overfitting when the network learns high variance functions to represent the training data. Data augmentation also helps to avoid overfitting and solve the imbalance problems in the images. Sometimes Convolution Neural networks cannot perform well so, we use augmentation techniques to solve these problems. It is the technique to expand the size of the original data and make the model more robust. The performance of the model is more accurate and works efficiently by applying the test time augmentation (TTA) and is dependent on how the image's weights are parametrized and learned After using some augmented techniques including random brightness, CLAHE, random flips, cropping, jittering, and blurring which are shown in figure 9.

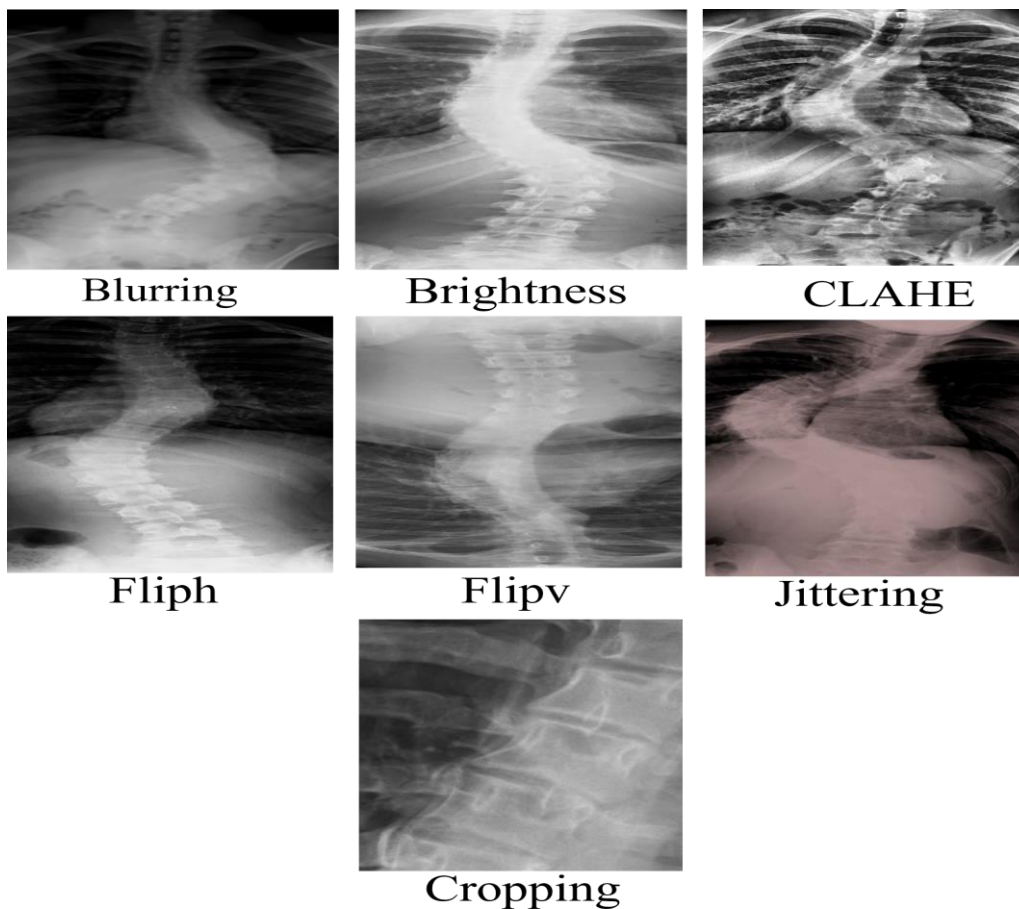


**Figure 9:** Spinal Augmented x-rays images

### 4.3 EfficientNet Model B4

To achieve the family models, a neural architecture search created the EfficientNet, a novel scale-up baseline network. In our work, the family model that spans from B0 to B7 is called EfficientNet, and we use it for training. This approach applies to classification issues and computer vision tasks, depending on the number of factors. ConvNets were developed before EfficientNet to customize the computation resources and scale up their dimensions. After some point, the depth of CNN scaled up, creating vanishing gradient problems, and making the model performance very low. To overcome this problem ResNet is used for the skipping connection. But for some reason, ResNet tells accurate information about depth, width, and resolution, but it also required manual fine-tuning. However, EfficientNet is used in our classification work which provides more and better accuracy than previous ConvNets.

This paper [45] presented the method of systematically scaling to represent the balancing of depth, width, and resolution of the convolutional neural network, which tends to lead to good performance. Depth, width, and resolution depend on each other under different conditions. Many ConvNet employ the depth scaling method to add more layers and extract more information from the data. The resolution of the neural network often increases as the depth does as well. While resolution scaling method provides high resolution in the input images, and it creates the pixel clear and more accurate to gain the fine-grained patterns from the image. A high-resolution image can provide more information, while less resolution means less information and it may create problems to identify the patterns. To extract more information from the image and make training easier, the width scaling method is employed for small-size models. It entails increasing the number of channels and being able to collect more fine-grained features. The authors proposed EfficientNet with the technique of compound scaling to balance all dimensions. Compound Scaling performs to balance the depth, width, and resolution as well. After the balancing of all dimensions, it improves the model's performance and accuracy. EfficientNet B4 training parameters are mentioned in table 2.

**Table 2:** EfficientNet B4 training parameters

Model	Training Parameters
<b>EfficientNet-B4</b>	<b>17,684,570</b>

### 4.3.1 Compound Scaling

Compound scaling, which recognizes that all multiple scaling dimensions are not independent, is the core goal of EfficientNet. Increasing the network depth will result in the image's greatest resolution. To balance all the dimensions to gain an accurate ratio. While this ratio is evaluated by the  $\alpha$ ,  $\beta$ ,  $\gamma$ . The overall compound scaling method is shown in figure 10.

Depth  $d$ :  $\alpha^\phi$

Width  $w$ :  $\beta^\phi$

Resolution  $r$ :  $\gamma^\phi$

$$F = \alpha \cdot \beta^\phi \cdot \gamma^\phi$$

$$F = d \cdot w^\phi \cdot r^\phi$$

Compound scaling works to scale up the number of layers, channels, and resolution as well. In the paper [45] authors have fixed the issues of the values of these dimensions  $\alpha$ ,  $\beta$ ,  $\gamma$  with help of a grid search. They also changed the coefficient value to scale up the next levels models  $\phi$ . By providing the values of coefficients by the following digits.

$$\alpha = 1.2$$

$$\beta = 1.1$$

$$\gamma = 1.5$$

under the constraint of  $\alpha \cdot \beta^2 \cdot \gamma^2 \approx 2$

Obtaining the constant values of the dimensions  $\alpha$ ,  $\beta$ , and  $\gamma$  means that the resolution of the image is increased by 15% then the width increases by 10%, and the depth by 20%. While depends on the data, the value of the coefficient  $\phi$  will be changeable to scale up the model and make it more perfect. A grid search is performed to identify the coefficient value  $\phi$ .

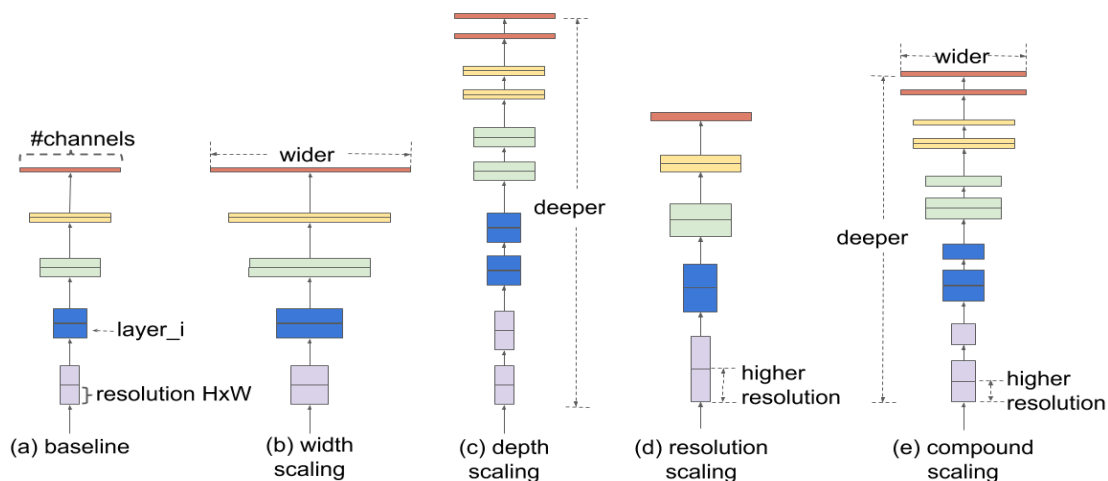
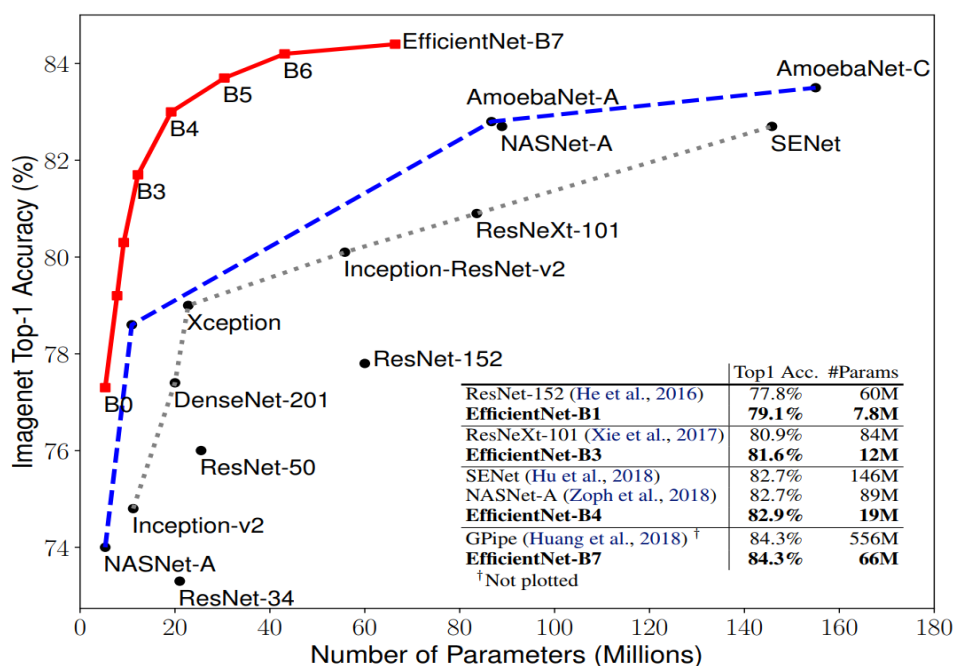


Figure 10: Compound Scaling [45]

### 4.3.2 Working of EfficientNet

EfficientNet results evaluated the scaling method with the existing of ConvNets and compared the results. As compared to the other single scaling method EfficientNet improves all-time accuracy. EfficientNet is a light-weighted model, and its FLOPS and parameters are very fewer than compared to the other models of ConvNet. It provides the efficiency and desired accuracy for a large scale of datasets and is also suitable for phone devices. EfficientNetB7 achieved accuracy on ImageNet of 84.4%, ranking first, and top-5 accuracy of 97.1% with 66M parameters and 37B FLOPS, respectively. Compared to earlier versions, EfficientNet is 8.4x smaller, 6.1x faster, and more accurate.

The EfficientNet-B1 outperforms ResNet-152 by 5.7 times. EfficientNet-B3 also achieved higher accuracy than ResNeXt-101 by using 18x fewer FLOPS. While EfficientNet-B4 performs the same number of FLOPS as the ResNet-50 by providing the top-1 accuracy which is 76.3%. In contrast to the alternative scaling technique, which offers great accuracy at the expense of additional FLOPS but is just as efficient as the baseline network, EfficientNet-B0. The compound scaling method improves the highest accuracy 2.5% as compared to single dimension methods. The state-of-the-art accuracy is provided in 5 out of 8 datasets by EfficientNet models, which are 9.6x more accurate than their predecessors' models. The compound scaling method provides more information and object details while other models are unable to get region information.



**Figure 11:** Accuracy and Working of EfficientNet Models [45]

### 4.3.3 EfficientNet's architecture with MBConv

Compound scaling's effectiveness is dependent on the baseline network. Performing neural architecture search (NAS) to create a new baseline network using the AutoML MNAS framework, which provides more accuracy and efficiency, will improve performance even further (FLOPS). In the architecture that resulted, Mobile Inverted Bottleneck Convolution (MBConv), which is identical to MobileNetV2 and MnasNet, was used. It has grown a small amount as a result of the FLOP budget expansion. Figure 12 depicts the EfficientNet-B0 design.

Starting from the EfficientNet-B0 baseline network, applied two steps for the compound scaling method to scale it up which are mentioned below.

- **Step 1:**

In the first step, fixing the value by  $\phi=1$  with assuming more resources available behind this by providing the grid search of  $\alpha$ ,  $\beta$ ,  $\gamma$ . After doing that process the authors found the values  $\alpha=1.2$ ,  $\beta=1.1$ ,  $\gamma=1.15$  under the constraints  $\alpha \cdot \beta^2 \cdot \gamma^2 \approx 2$  which is mentioned above as well.

- **Step 2:**

The authors fixed the constraints  $\alpha$ ,  $\beta$ , and  $\gamma$  values to scale up the baseline with different values  $\phi$  to get the EfficientNet-B1 to EfficientNet-B7.

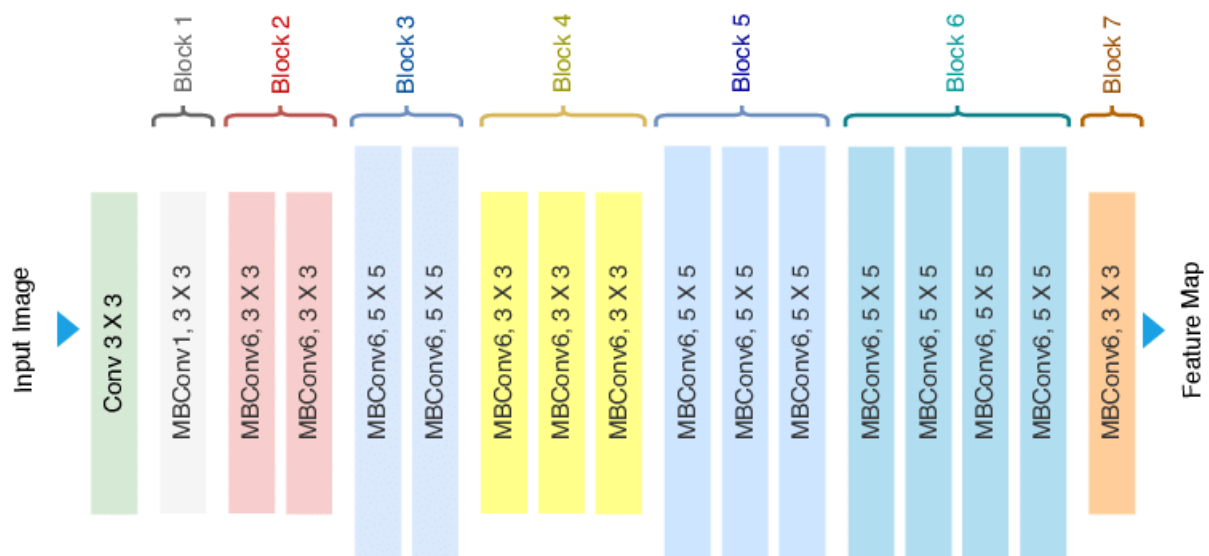


**Figure 12:** Architecture of EfficientNet with MBConv

### 4.3.4 ImageNet results for EfficientNet

EfficientNet uses the same procedure described above to operate on ImageNet. RMSProp optimizer with a momentum of 0.99 and fading of  $0.9 \times 10^{-5}$  weight deteriorates while the initial learning rate is 0.56 and corrosion increases by 0.97 every 2.54 epochs. Generally, bigger models need more regularization. The authors [45] increased the dropout ratio of EfficientNet-B0 to 0.2 and it reached 0.5 for EfficientNet-B7. These models, which are not small but also computationally less expensive, are employed for orders of magnitudes with fewer parameters than other models that provide the same precision. To evaluate the cost measured the inference latency on the CPU and provide the latency average report by over 20 runs. However, additionally quick and usable with real hardware is EfficientNet.

### 4.3.5 Results of Transfer Learning for EfficientNet

Evaluating the EfficientNet on the transfer learning datasets. Compared the accuracy and results of the NASNet-A, and Inception-v4. EfficientNet performs high accuracy with a 4.7x average parameters reduction. Different publicly available datasets and different models are applied like DAT which obtains the dynamically training data and GPipe which is specialized for pipeline parallelism. Some of the datasets are mentioned below in table 3 with their accuracy. Compared to other models like ResNet, DenseNet, Inception, and NasNet, the EfficientNet model performs better with fewer parameters.

**Table 3:** EfficientNet Performance Results on Transfer Learning Datasets [45]

	Model	Comparison to best public-available results				
		Acc.	#Param	Our Model	Acc.	#Param(ratio)
CIFAR-10	NASNet-A	98.0%	85M	EfficientNet-B0	98.1%	4M (21x)
CIFAR-100	NASNet-A	87.5%	85M	EfficientNet-B0	88.1%	4M (21x)
Birdsnap	Inception-v4	81.8%	41M	EfficientNet-B5	82.0%	28M (1.5x)
Stanford Cars	Inception-v4	93.4%	41M	EfficientNet-B3	93.6%	10M (4.1x)
Flowers	Inception-v4	98.5%	41M	EfficientNet-B5	98.5%	28M (1.5x)
FGVC Aircraft	Inception-v4	90.9%	41M	EfficientNet-B3	90.7%	10M (4.1x)
Oxford-IIIT Pets	ResNet-152	94.5%	58M	EfficientNet-B4	94.8%	17M (5.6x)
Food-101	Inception-v4	90.8%	41M	EfficientNet-B4	91.5%	17M (2.4x)
Geo-Mean						<b>(4.7x)</b>



## 4.4 GAP Layer (Global Average Pooling)

After the implementation of the EfficientNet, Global Average Pooling was used to evaluate the average value. It applies the average pooling on the spatial dimensions, and it produced the output of a single map feature. For generating one feature map corresponding to each classification task. It can decide to take the base average of each feature map instead of adding a connected layer on top of them, and the resulting vector can then be directly fed into the SoftMax layer, which prides the results on the probability. In short GAP layers are used for the reduction of dimensions of the output layer and provide to overcome the overfitting of the model. Another advantage is that there is no parameter to train for the GAP layer. It helps to provide localization and object detection. In our work, the final layer is Global Average pooling, and the last and output layer is the SoftMax layer.

## 4.5 SoftMax Activation Layer

SoftMax is the function that the values can be obtained from 0 to 1. The input values can be positive, negative, zero, and other, while SoftMax converted these values into a sum of 0 to 1. So, it is interpreted as the probabilities. If one is in negative or small value, then it SoftMax converts into small probability while in positive output then turns into large probability. It will always remain in 0 or 1. In some cases, SoftMax is called Softargmax. Being used for multiclass classification makes it a generalization of logistic regression. The sigmoid function, which is also employed in logistic regression, has a formula that is like SoftMax. When classes are mutually exclusive, it is only utilized for classification. A normalized probability distribution is provided in part by SoftMax, which can also be displayed to users and utilized as input by other systems.

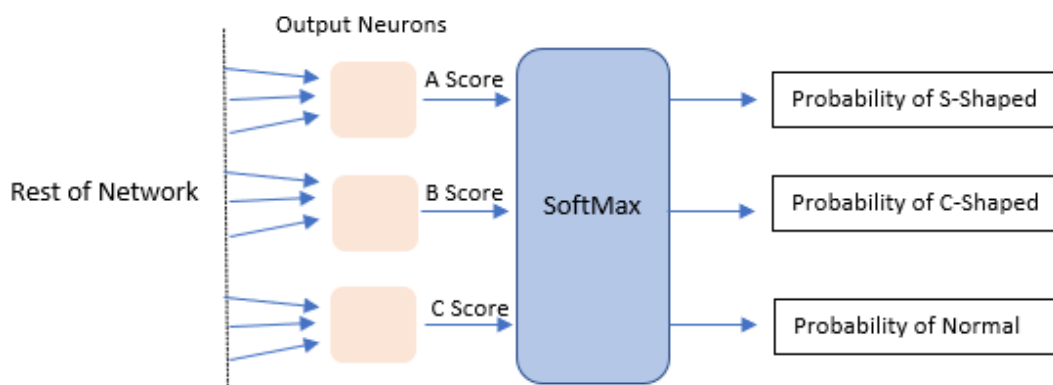


**Figure 13:** SoftMax Activation Function

## 4.6 Loss Function

Loss function reacts as evaluating method of the Machine learning algorithms for feature datasets. During the training phase, the loss function optimizes the model and is directly related to its prediction. The main objective is to minimize the loss function since the model functions better when the loss function value is low. To enhance the model performance needs to decrease the loss function and improve results. The loss function measured the model performance in terms of predicting expected outputs. It majors into two categories. In first is classification, which predicts the probabilities of all classes, while regression predicts the continuous value which is a given set of independent features.

### 4.6.1 Sparse Categorical Cross Entropy

In this study, Sparse Categorical Cross Entropy is used to calculate the values between probability and truth values. Truth values for the three classes—Normal, S-shaped, and C-shaped—are encoded using cross-entropy.

Each predicted output is compared with the actual class and evaluated the loss which is based on the probabilities. If the loss is large then is close to 1, and if the loss is small then it is close to 0. It is used for the model weights during the training phase. The smaller loss provides better results, while the large loss provides bad results. Cross entropy loss 0 if the model performs excellently.

- **Cross Entropy is characterized by:**

$$Lce = - \sum_{i=1}^n t_i \log(p_i), \quad \text{for } n \text{ classes}$$

Where  $t_i$  is the actual class

$p_i$  is the softmax probability for the  $i^{th}$  class

Sparse Categorical Cross Entropy is used in this work which is also mentioned above because our problem is multi-class where the output is labeled assigned in the integer (0,1,2, 3..) values. It has the same loss function with categorical cross entropy, but a different interface.

## 4.7 Optimizer

Adam optimizer used in our experiment is used to produce the updated network weights of the training data. For model optimization with the initial learning rate, the adaptive momentum of the estimate is 0.001. Adam, a popular optimizer, is created by combining Adagrad and RMSProp. Adagrad maintains the pre-parameters learning rate to provide the best performance and keeps the average of the past gradient and it works better in sparse gradient as well. while RMSProp also maintains the pre-parameters learning rate which is based on the adaptive and provides the recent average magnitudes of the gradient for the weights and is also used for the online settings. Both are used for large-scale computer vision tasks It is the extended version of the Gradient Descent. Adam optimizer was tested on the MNIST dataset which is shown below in figure 14.

The authors [69] provide the default settings of Adam:

$\alpha$  represent alpha,  $\beta_1$  represents beta1,  $\beta_2$  represents beta2, and  $\epsilon$  represent epsilon.

$\alpha = 0.001$ ,  $\beta_1 = 0.9$ ,  $\beta_2 = 0.999$  and  $\epsilon = 10^{-8}$

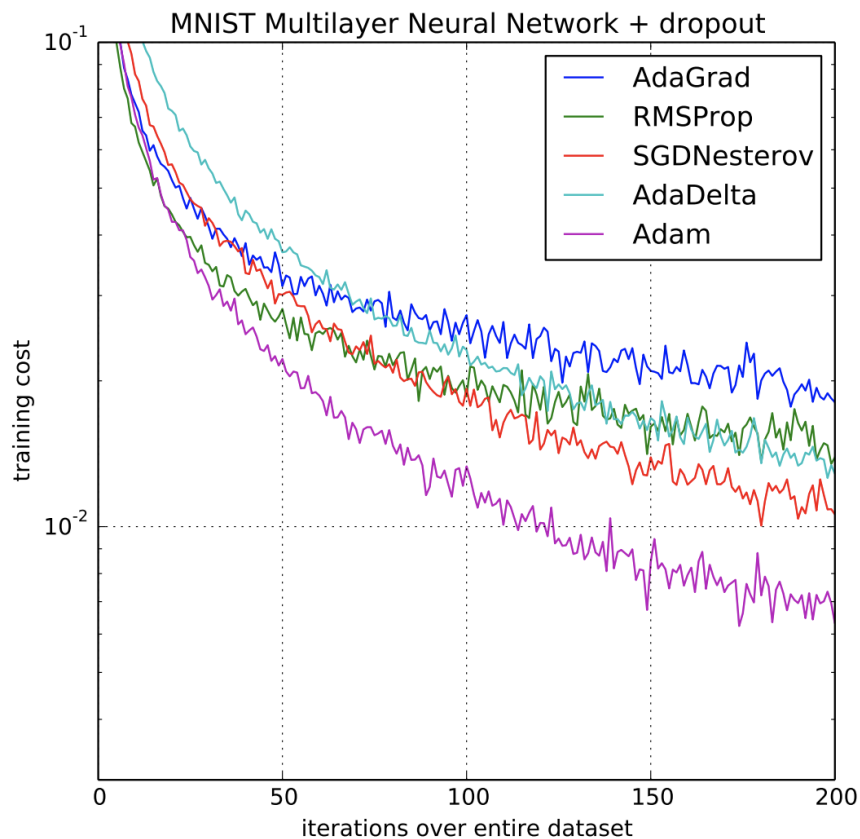


**Figure 14:** Adam Optimizer Algorithm [69]

## 4.7 Transfer Learning

Transfer learning is flexible, and it allows the director to the pre-trained models for the preprocessing, feature extraction, and integration with the new models. Transfer learning involves the problems of the trained model and involves the starting point of the other related model. One or more layers are used of the trained model for the next problem if the problem is related to it. Because the training model requires random weight initialization and weight adjustments take a long time, we have used pre-trained weights on the ImageNet dataset in our research. We employed ImageNet's trained model in our work to resolve this issue. Transfer learning helps to provide the train model weights to make training fast and easier to debug. In ImageNet there are 1000 classes to predict while in our work there are only 3 to classify. The pre-trained model for classifying and predicting classes is connected to the SoftMax layer. For the prediction of three classes in our work, we included the Global Average Pooling (GAP) layer with the SoftMax layers. These layers were well trained and fine-tuned to accommodate their weights to classify the classes using backpropagation. That's the reason transfer learning provides accurate models in a time-saving way, and it is very popular in computer vision tasks.

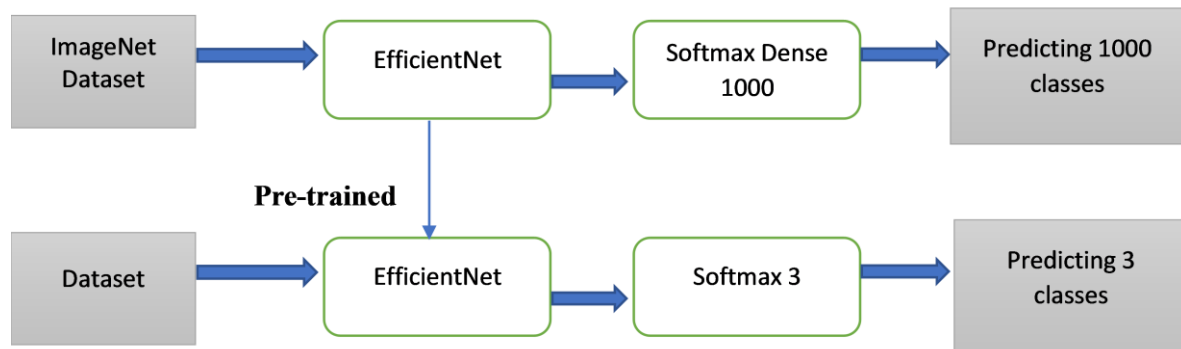


**Figure 15:** Transfer Learning Technique

## 4.8 Pipeline and Experimental Setup

In our dataset, their spine X-ray images are involved in different shapes and sizes, like S-shaped, C-Shaped, and Normal. First, load the images, and used the pre-trained model of EfficientNet-b4. Images are not directly loaded into the EfficientNet. It has required a fixed image size of 380\*380. After loading the image, we applied the augmentation technique to explore the images in different ways. Data augmentation is applied in our model to make it more robust, avoid overfitting and solve the issues of imbalance objects. However, the dataset was scaled by 380\*380 and then augmented. Our approach is built on TensorFlow [70] by training the deep learning model. Then, we utilized Adam Optimizer with a 0.001 learning rate initially. Finally, employed GAP Layer and SoftMax Layer to forecast the classes. Some parameters are shown in table 4 which are applied in our experiment.

**Table 4:** Parameters Detail

Model	EfficientNet-B4
Input size	380*380
Optimizer	Adam
Initial Learning Rate	0.001
Activation	SoftMax
Epochs	50
Total training Parameters	17,684,570

The overall propped methodology is shown in figure 16 which is already mentioned above in detail. First, loads the data for pre-processing step then apply augmented techniques to obtain large-scale data with different shapes and sizes. After this applied EfficientNet Model to the augmented dataset. GAP layers are used to minimize the dimensions in the output layer. Finally, these output layers passed through the SoftMax activation function, while this layer predicts the classification in a probability way.

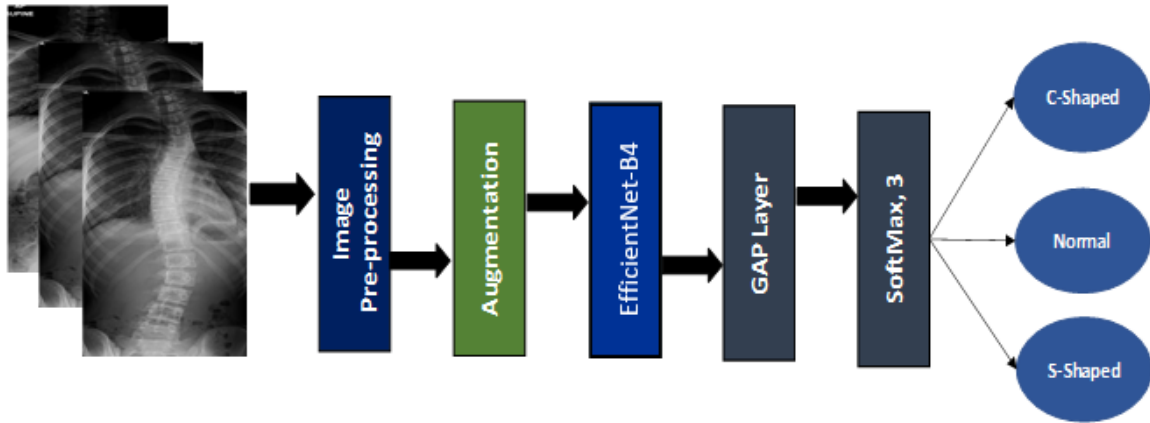


**Figure 16:** Pipeline of Proposed Methodology

In chapter 4, we proposed the methodology for the automatic detection and classification of scoliosis from x-rays images using transfer learning. In our framework, we used the EfficientNet-B4 for scoliosis categorization. It is used to extract features from x-ray images of the spine. Data Techniques for augmentation are used to enhance the quality and various scales of images. It helps to avoid overfitting problems and solve class imbalance and explore the object. After we compared the results before and after the augmentation techniques. We have three classes in our dataset, and we achieved class-wise accuracy in the three classes. GAP layer and SoftMax are used to predict the probabilities of each class which are always between 1 and 0. With a 0.001 learning rate initially, we employed Adam Optimizer. The values between the probability and truth values have been assessed using sparse cross-entropy. The truth values for the three classes Normal, S-shaped, and C-shaped are encoded in cross-entropy. In addition, we have used Transfer learning techniques to maintain the weight of the training model, and it helps the model be smoother and easier to debug. We used the ImageNet weights to predict the classes. Transfer learning accommodates the training model in a very limited time, and it is very popular in computer vision tasks. Our work is built on deep learning models, and we use the Kaggle platform to apply the training to TensorFlow. Our approach is built on the TensorFlow-trained deep learning model, which is extensively covered in this chapter. After applying these methods in our experiences, we get an accuracy of 89% for the classification of scoliosis (Normal, S-Shaped, C-Shaped). Before the augmentation technique, we achieved an accuracy of 76%. However, after augmentation, we achieved the best results to improve the accuracy by 13%.

## CHAPTER 5: EXPERIMENTAL RESULTS

### 5.1 Dataset

The dataset for the proposed methods includes 609 anterior-posterior x-ray images from the publicly accessible Accurate Automated Spinal Curvature Estimation 2019 Grand Challenge. This dataset contains multiple images of spine x-rays like S-Shaped, C-Shaped, and Normal. In our dataset 454 images are used to predict the classification and randomly split the data into 80:20 across train and validation.

#### 5.1.1 AASCE 2019 Dataset

We have 454 images as mentioned above and these images are categorized into three classes. These three categories have multiple images, 308 X-ray images contain in the S-Shaped curve, which is the abnormal curve, 128 X-ray images contained in the C-Shaped curve, and 18 X-ray images contained in the Normal curve. We scale up the dataset for the EfficientNet model by 380\*380. The dataset consists of multiple sizes in jpg format. Some random images are selected for the X-rays which are shown in figure 17.

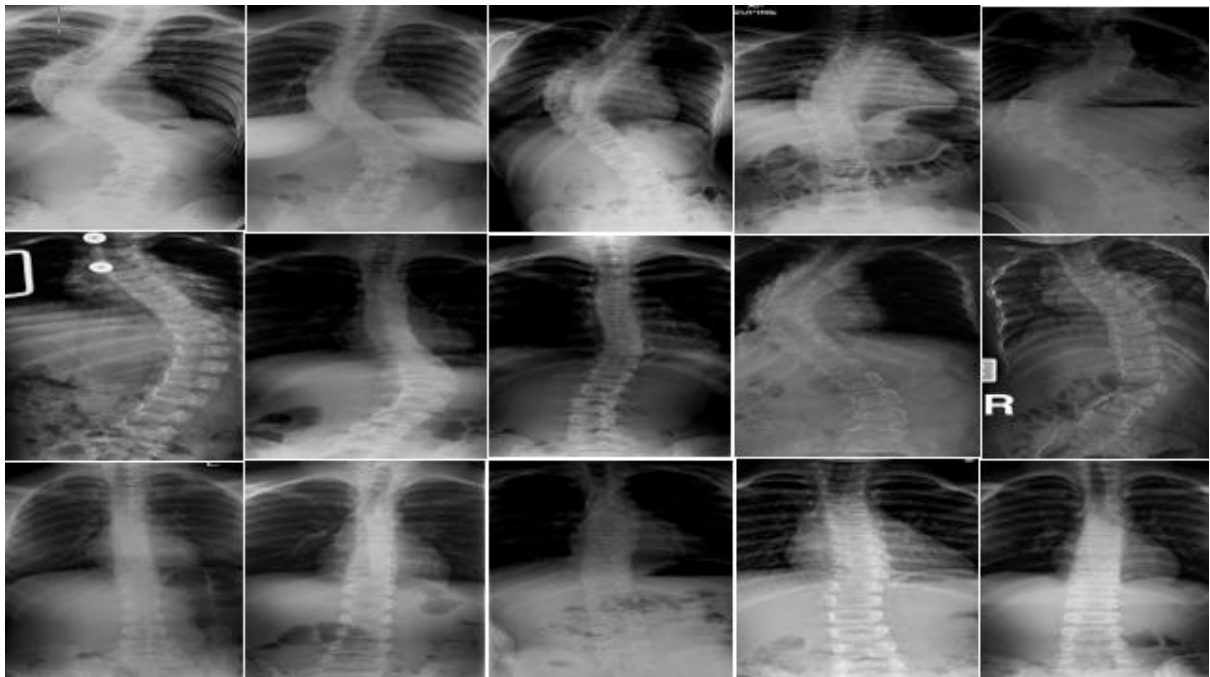


**Figure 17:** Randomly Images Selected from Spine X-rays

## 5.2 Performance Evaluation

The performance of the model can be determined using the standard parameters. We also employed sensitivity (SEN) and specificity (SPE) measurements in our multiclass problem. When discussing the index, Specificity and Sensitivity are sometimes said to overlap, as is the True Positive Rate (TPR) and True Negative Rate. The parameters are all displayed below.

$$SEN = TPR = \frac{TP}{TP + FN} \quad (5.1)$$

$$SPE = TNR = \frac{TN}{TN + FP} \quad (5.2)$$

$$FPR = 1 - SPE = \frac{FP}{FP + TN} \quad (5.3)$$

$$ACC = \frac{TP + TN}{TP + TN + FP + FN} \quad (5.4)$$

These parameters are crucial for producing the results of the normal and abnormal curves in our multiclass issues.

In case of Classification:

- TP produced the number of abnormalities (S-Shaped, C-Shaped) from Spine X-rays Images that were appropriately labeled abnormal.
- FP generated normal spine X-ray images that were incorrectly labeled as abnormal.
- TN represents the quantity of correctly detected normal spine x-rays.
- FN is the quantity of spine X-ray abnormalities that are mistakenly labeled as normal.
- TPR generated the positives that were correctly classified, which are divided by the total number of positives.
- FPR assesses the positives that were incorrectly identified and divides the total number of negatives.



## 5.2 Results

### 5.2.1 Results of the EfficientNet model's classification without augmentation

The classification methodology was evaluated on the local dataset. In this dataset, we achieved an accuracy of 76%. After that, we use the Data Augmentation technique to improve the accuracy by 89%. Table 5 shows the overall work of the experiment in which the EfficientNet model was used for the classification but achieved accuracy without Augmentation and figure 18 shows the confusion matrix without Augmentation. Table 6 shows the structure of the experiment with the augmentation technique.

**Table 5:** Overall Structure of experiment without Augmentation

Model	Training parameters	Optimizer	Augmentation	Loss function	Accuracy (ACC)
EfficientNet-B4	17,684,570	Adam	No	Sparse Categorical Cross Entropy	76%

Our multi-class classification problem is a three-class classification problem. We have a dataset in which three classes occur double (S-shaped), single (C-shaped), and Normal. The following is the possible confusion matrix of three classes without augmentation.

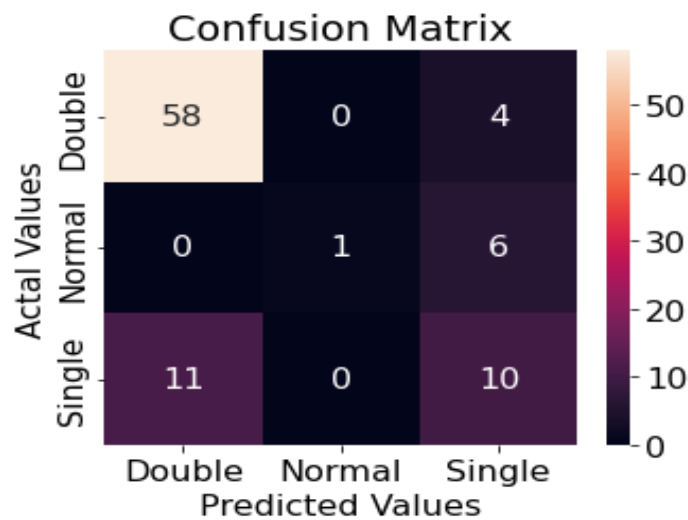


**Figure 18:** Confusion Matrix of EfficientNet without Augmentation

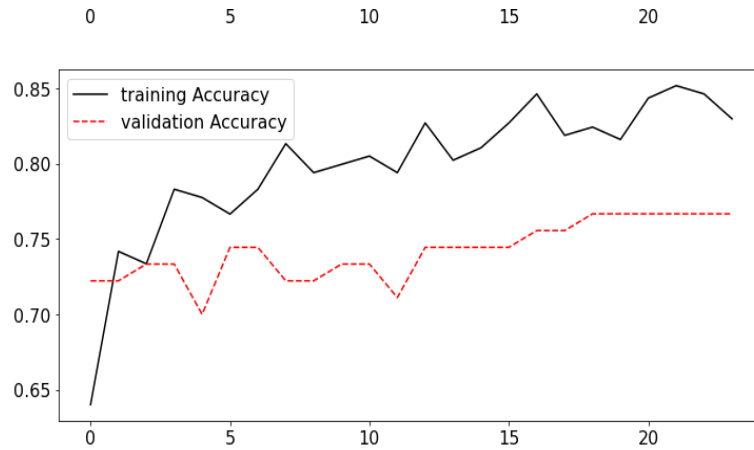


**Figure 19:** Learning Curves without Augmentation

### 5.2.2 Results of the EfficientNet model's classification with augmentation

It enhanced the model's performance and improved the accuracy by 13%. In Data Augmentation random flip, random brightness, and blurring techniques are used to improve the quality and noise problems in the images. The overall structure is explained in table 6 and shown the confusion matrix with augmentation is shown in figure 20.

**Table 6:** Overall Structure of experiment with Augmentation

Model	Training parameters	Optimizer	Augmentation	Loss function	Accuracy (ACC)
EfficientNet-B4	17,684,570	Adam	Yes	Sparse Categorical Cross Entropy	89%

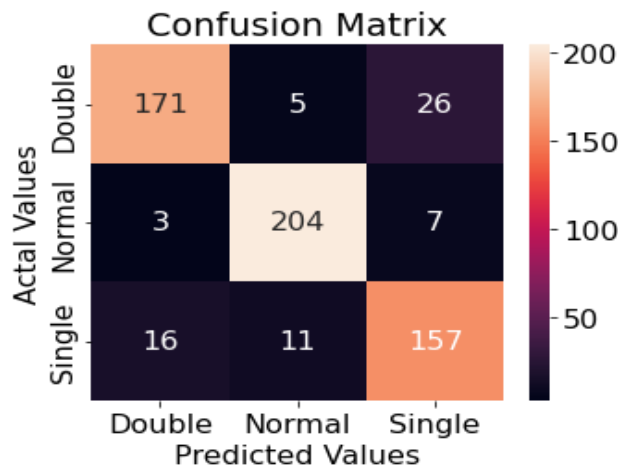


**Figure 20:** Confusion Matrix of EfficientNet with Augmentation

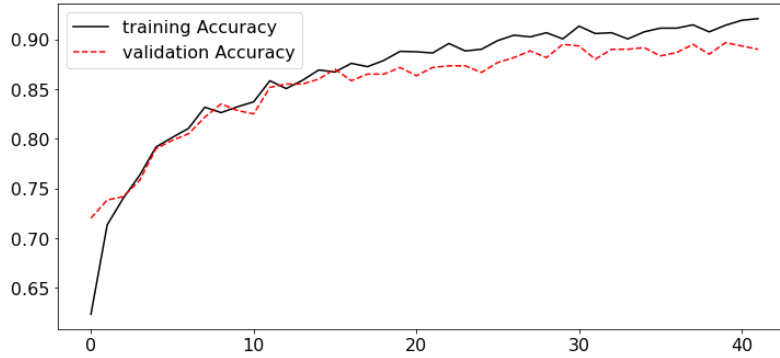


**Figure 21:** Learning Curves with Augmentation

As shown in figure 21, the learning curves for validating accuracy during training and using augmented data. First, we set the epochs between 40 to 50, and the model was set on the 0.001 learning rate. But we have achieved the highest accuracy between 35 to 40 epochs with the best accuracy of 89%. The model was restored for the best epochs and where we get the loss is minimum. After that our model still trained after the highest point but did not achieve accuracy after that. Learning curves of EfficientNet-B4 show that validation accuracy reaches the training accuracy, while it reduced model overfitting issues.

### 5.2.3 Classification Accuracy with and without Augmentation

- **S-Shaped Accuracy**

In S-Shaped we have 62 images before the augmentation then we achieved an accuracy of 0.93 due to the small data and it produced better results. After the augmentation technique, images increased by 202 and it produced an accuracy of 0.84 which is shown in table 7.

- **C-Shaped Accuracy**

In C-Shaped, we have 21 before the augmentation, apply the classification models, and achieved the results with an accuracy of 0.47, and after the augmentation achieved the accuracy of 0.85 with 184 images which are shown in table 7.

- **Normal Accuracy**

In a normal dataset, we have 7 images, applied the classification models, and achieved the results with an accuracy of 0.14 because due to the lack of data, after the augmentation, we have achieved the accuracy of 0.95 with 214 images which are shown in table 7.

**Table 7:** Class-wise Accuracy with and without Augmentation

Class	Accuracy without Augmentation	Accuracy with Augmentation
S-Shaped	0.93	0.84
C-Shaped	0.47	0.85
Normal	0.14	0.95

The comparison of our technique with other different techniques on anterior-posterior x-ray images from the publicly accessible Accurate Automated Spinal Curvature Estimation 2019 Grand Challenge.

**Table 8:** Comparison of AASCE 2019 (SMAPE and ACCURACY)

Year	Author	Technique	Accuracy (ACC) (%) / SMAPE
2021	J.-L. Cui et al [3]	U-net network	(SMAPE) is 21.675%,
2019	S. Wang et al [63]	SCG-Net	22.1775 is SMAPE
2022	A. Amin et al [67]	EfficientNet-B7	0.86% ACC
2022	W. Caesarendra et al [68]	Convolution Neural Network	0.90% ACC
2019	B. Khanal et al [39]	Faster-RCNN + DenseNet	SMAPE is 25.69
2019	R. Tao et al [40]	ResNet50 + FPN + FCN	SMAPE is 25.4784
<b>2022</b>	<b>Ours</b>	<b>EfficientNet-B4</b>	<b>0.89% ACC</b>

## Discussion

The results indicate that an impressive contribution of Efficient-B4 must detect and classify scoliosis from spine x-rays images. The research in this instance is broken down into two stages. Without using an additional dataset, the first phase uses the EfficientNet model built on ConvNet to categorize the spinal curvature. In another step, data augmentation used to become large amount it has been utilized for the classification problem makes the model performs well. While after the augmentation technique we found an improvement of 13% in our accuracy. We decided to use augmented techniques like random brightness, random flip, and blurring. We used the augmentation strategy while keeping the optimum hyperparameters for each model. It is preventing the model overfits. The results of the augmented dataset were analyzed through the EfficientNet model and produced better results. Although the literature shows good results with the usage of CNN, ResNets, U-Net, and Faster RCNN but those papers hybrid and modified versions to refine the classification problem and segmentation as well.

The challenge of the dataset was to introduce the approach of the S and C shape curvature of classification scoliosis. The EfficientNetB4-based approach cannot be used as comparative as other research before. By using this approach, we achieved class-wise accuracy with and without augmentation. This method is reasonable from a clinical standpoint because there are three classifications for scoliosis (Normal, S-Shaped, and C-Shaped). The treatment method might be similar for the S and C curvature like physical therapy, massage, surgery, and braces. The curvature needs to be identified by these treatments. S-Shaped curvatures are more dangerous than others because it has two curvature sides. While some researchers also worked on then Cobb's angle estimation, it is useful when no further option is remaining except surgery. While it is the pre-operative method, in our approach we proposed the early diagnosis of scoliosis and shape-based deformity classification which provide help for the treatment prescriptions from medical experts. That is why after the classification of scoliosis medical experts confirm the deformity of the spine in which condition it exists. Classification of scoliosis is very useful as compared with other manual diagnoses.

## **CHAPTER 6: CONCLUSION AND FUTURE WORK**

### **6.1 Conclusion**

The findings demonstrate that trained EfficientNet-B4 is the most effective method for identifying and categorizing scoliosis (S-Shaped, C-Shaped, Normal). Our trained model helps to predict the analysis of scoliosis disease in the medical field. Medical experts will use this tool to interpret the experiment with help of a computer machine and it will give the results in seconds. Moreover, in our experiment, we used data augmentation techniques and compare the results before and after augmentation. After augmentation, we achieved more accuracy than before by a 13% increase. While we achieved the class-wise accuracy (S-Shaped, C-Shaped, Normal) with and without augmentation. It helps to avoid overfitting problems and makes the model more robust and easier to evaluate. While to speed up the training model, we used already pre-trained weights that are implemented in the ImageNet dataset. In terms of training the model, it requires the random initialization weights, but it consumes more time to adjust their weights. To overcome this situation, we used pre-trained weights to make the model faster and computationally cheap. However, Transfer learning is crucial for accelerating the learning process and improving the model's generalizability and debuggability. Trained model of ImageNet dataset used in our local dataset at the initial position. In the end GAP and SoftMax layers were applied to classify the classes in the probability process which is between 0 and 1.

### **6.2 Contribution**

Major contributions of this research are:

- Proposed a fully automatic system for scoliosis from x-rays images and classification of scoliosis using the EfficientNet.
- Applied Augmentation techniques and compare the results before and after the augmentation.
- Reviewed and compare the already techniques which are used in the detection and classification of scoliosis
- Achieved higher accuracy in the classification of the AASCE dataset.

## **6.2 Future Work**

With the development of machine learning algorithms, manually features are selected, and the classifier is trained on them. On the other hand, a deep learning model is adequate to extract the features. However, the transfer learning approach model we utilized in our work will assist in the future in extracting the useful features and readily transferring them to any other tasks involving spine x-rays. With a small amount of change, the suggested methodology can be applied to various categorization problem tasks.

## REFERENCES

- [1] P. D. Nachum Dafny. "Chapter 3: Anatomy of the Spinal Cord." <https://nba.uth.tmc.edu/neuroscience/s2/chapter03.html> (accessed.
- [2] "S And C-Shaped Scoliosis Differences, Causes & Best Treatment." <https://skoliosis.my/spinal-curves/s-shaped-scoliosis-c-shaped-scoliosis/> (accessed.
- [3] J.-L. Cui, D.-D. Gao, S.-J. Shen, L.-Z. Wang, and Y. Zhao, "Cobb Angle Measurement Method of Scoliosis Based on U-net Network," 2021.
- [4] J. Shen *et al.*, "Towards a new 3D classification for adolescent idiopathic scoliosis," *Spine Deformity*, vol. 8, no. 3, pp. 387-396, 2020.
- [5] S. K. Wardani, R. Sigit, S. M. S. Putri, and D. Yunitasari, "Measurement of Spinal Curvature for Scoliosis Classification," in *2018 International Seminar on Application for Technology of Information and Communication*, 2018: IEEE, pp. 266-270.
- [6] M. R. Konieczny, H. Senyurt, and R. Krauspe, "Epidemiology of adolescent idiopathic scoliosis," *Journal of children's orthopaedics*, vol. 7, no. 1, pp. 3-9, 2013.
- [7] C.-W. J. Cheung, G.-Q. Zhou, S.-Y. Law, T.-M. Mak, K.-L. Lai, and Y.-P. Zheng, "Ultrasound volume projection imaging for assessment of scoliosis," *IEEE transactions on medical imaging*, vol. 34, no. 8, pp. 1760-1768, 2015.
- [8] S. Banerjee, S. H. Ling, J. Lyu, S. Su, and Y.-P. Zheng, "Automatic segmentation of 3d ultrasound spine curvature using convolutional neural network," in *2020 42nd Annual International Conference of the IEEE Engineering in Medicine & Biology Society (EMBC)*, 2020: IEEE, pp. 2039-2042.
- [9] W. H. Organization. "Spinal Cord Injury " <https://www.who.int/news-room/fact-sheets/detail/spinal-cord-injury> (accessed.
- [10] "TREATMENT THROUGH THE CENTURIES." <https://www.align-clinic.com/blog/the-history-of-scoliosis-treatment-through-the-centuries> (accessed.
- [11] B. A. Frost, S. Camarero-Espinosa, and E. J. Foster, "Materials for the spine: anatomy, problems, and solutions," *Materials*, vol. 12, no. 2, p. 253, 2019.
- [12] T. A. o. t. T. Spine. "The Anatomy of the Thoracic Spine." <https://www.verywellhealth.com/thoracic-spine-297288> (accessed.
- [13] B. S. J. D. Carrier. "Anatomy, Back, Lumbar Spine." <https://www.ncbi.nlm.nih.gov/books/NBK557616/> (accessed.



- [14] R. Brouhard. "The Anatomy of the Sacrum." <https://www.verywellhealth.com/sacrum-anatomy-4587600> (accessed).
- [15] R. Staehler. "Anatomy of the Coccyx (Tailbone)." <https://www.spine-health.com/conditions/spine-anatomy/anatomy-coccyx-tailbone> (accessed).
- [16] I. Karpiel, A. Ziębiński, M. Kluszczynski, and D. Feige, "A Survey of Methods and Technologies Used for Diagnosis of Scoliosis," *Sensors*, vol. 21, no. 24, p. 8410, 2021.
- [17] G. Q. Z. Wei Wei Jiang , Ka Lee Lai , Song Yu Hu , Qing Yu Gao , Xiao Yan Wang , Yong Ping Zheng "A fast 3-D ultrasound projection imaging method for scoliosis assessment." <https://pubmed.ncbi.nlm.nih.gov/30947409/> (accessed).
- [18] H. Kuroki, "Brace treatment for adolescent idiopathic scoliosis," *Journal of clinical medicine*, vol. 7, no. 6, p. 136, 2018.
- [19] S. Johnson. "Everything You Need to Know About Scoliosis." <https://www.healthline.com/health/scoliosis> (accessed).
- [20] M. Bialek and A. M'hango, "" FITS" concept Functional Individual Therapy of Scoliosis," *Studies in health technology and informatics*, vol. 135, pp. 250-261, 2008.
- [21] C. Coillard, A. Circo, and C. H. Rivard, "A new concept for the non-invasive treatment of Adolescent Idiopathic Scoliosis: The Corrective Movement© principle integrated in the SpineCor system," *Disability and Rehabilitation: Assistive Technology*, vol. 3, no. 3, pp. 112-119, 2008.
- [22] J. Bettany Saltikov, E. Parent, M. Romano, M. Villagrasa, and S. Negrini, "Physiotherapeutic scoliosis-specific exercises for adolescents with idiopathic scoliosis," 2014.
- [23] M. Jelačić, M. Villagrasa, E. Pou, G. Quera-Salvá, and M. Rigo, "Barcelona Scoliosis Physical Therapy School–BSPTS–based on classical Schroth principles: short term effects on back asymmetry in idiopathic scoliosis," *Scoliosis*, vol. 7, no. 1, pp. 1-1, 2012.
- [24] M. Romano, A. Negrini, S. Parzini, and S. Negrini, "Scientific Exercises Approach to Scoliosis (SEAS): efficacy, efficiency and innovation," *Studies in health technology and informatics*, vol. 135, pp. 191-207, 2008.
- [25] H.-R. Weiss, "The method of Katharina Schroth-history, principles and current development," *Scoliosis*, vol. 6, no. 1, pp. 1-22, 2011.
- [26] H. Inoue, "Data augmentation by pairing samples for images classification," *arXiv preprint arXiv:1801.02929*, 2018.

- [27] L. Perez and J. Wang, "The effectiveness of data augmentation in image classification using deep learning," *arXiv preprint arXiv:1712.04621*, 2017.
- [28] B. Ma *et al.*, "Data augmentation in microscopic images for material data mining," *npj Computational Materials*, vol. 6, no. 1, pp. 1-9, 2020.
- [29] s. L. P. Aggarwal, "Data augmentation in dermatology image recognition using machine learning," *Skin Research and Technology*, vol. 25, no. 6, pp. 815-820, 2019.
- [30] A. Fawzi, H. Samulowitz, D. Turaga, and P. Frossard, "Adaptive data augmentation for image classification," in *2016 IEEE international conference on image processing (ICIP)*, 2016: Ieee, pp. 3688-3692.
- [31] T. Tran, T. Pham, G. Carneiro, L. Palmer, and I. Reid, "A bayesian data augmentation approach for learning deep models," *Advances in neural information processing systems*, vol. 30, 2017.
- [32] J. Shijie, W. Ping, J. Peiyi, and H. Siping, "Research on data augmentation for image classification based on convolution neural networks," in *2017 Chinese automation congress (CAC)*, 2017: IEEE, pp. 4165-4170.
- [33] A. Mikołajczyk and M. Grochowski, "Data augmentation for improving deep learning in image classification problem," in *2018 international interdisciplinary PhD workshop (IIPhDW)*, 2018: IEEE, pp. 117-122.
- [34] Q. Zheng, M. Yang, X. Tian, N. Jiang, and D. Wang, "A full stage data augmentation method in deep convolutional neural network for natural image classification," *Discrete Dynamics in Nature and Society*, vol. 2020, 2020.
- [35] S. Wickramanayake, W. Hsu, and M. L. Lee, "Explanation-based Data Augmentation for Image Classification," *Advances in Neural Information Processing Systems*, vol. 34, pp. 20929-20940, 2021.
- [36] S. Gu, M. Pednekar, and R. Slater, "Improve image classification using data augmentation and neural networks," *SMU Data Science Review*, vol. 2, no. 2, p. 1, 2019.
- [37] R. H. Alharbi, M. B. Alshaye, M. M. Alkanhal, N. M. Alharbi, M. A. Alzahrani, and O. A. Alrehaili, "Deep learning based algorithm for automatic scoliosis angle measurement," in *2020 3rd International Conference on Computer Applications & Information Security (ICCAIS)*, 2020: IEEE, pp. 1-5.
- [38] I. Obeid, P. Berjano, C. Lamartina, D. Chopin, L. Boissière, and A. Bourghli, "Classification of coronal imbalance in adult scoliosis and spine deformity: a treatment-oriented guideline," *European Spine Journal*, vol. 28, no. 1, pp. 94-113, 2019.

- [39] B. Khanal, L. Dahal, P. Adhikari, and B. Khanal, "Automatic Cobb angle detection using vertebra detector and vertebra corners regression," in *International Workshop and Challenge on Computational Methods and Clinical Applications for Spine Imaging*, 2019: Springer, pp. 81-87.
- [40] R. Tao, S. Xu, H. Wu, C. Zhang, and C. Lv, "Automated spinal curvature assessment from X-ray images using landmarks estimation network via rotation proposals," in *International Workshop and Challenge on Computational Methods and Clinical Applications for Spine Imaging*, 2019: Springer, pp. 95-100.
- [41] Z. He *et al.*, "Classification of neurofibromatosis-related dystrophic or nondystrophic scoliosis based on image features using bilateral CNN," *Medical Physics*, vol. 48, no. 4, pp. 1571-1583, 2021.
- [42] N. Sabri, H. N. A. Hamed, Z. Ibrahim, and K. Ibrahim, "2D Photogrammetry Image of Scoliosis Lenke Type Classification Using Deep Learning," in *2019 IEEE 9th International Conference on System Engineering and Technology (ICSET)*, 2019: IEEE, pp. 437-440.
- [43] Z. Tan *et al.*, "An Automatic Scoliosis Diagnosis and Measurement System Based on Deep Learning," in *2018 IEEE International Conference on Robotics and Biomimetics (ROBIO)*, 2018: IEEE, pp. 439-443.
- [44] S. Rothstock, H.-R. Weiss, D. Krueger, and L. Paul, "Clinical classification of scoliosis patients using machine learning and markerless 3D surface trunk data," *Medical & Biological Engineering & Computing*, vol. 58, no. 12, pp. 2953-2962, 2020.
- [45] M. Tan and Q. Le, "EfficientNet: Rethinking model scaling for convolutional neural networks," in *International conference on machine learning*, 2019: PMLR, pp. 6105-6114.
- [46] C. Vergari, W. Skalli, and L. Gajny, "A convolutional neural network to detect scoliosis treatment in radiographs," *International Journal of Computer Assisted Radiology and Surgery*, vol. 15, no. 6, pp. 1069-1074, 2020.
- [47] J. Yang *et al.*, "Development and validation of deep learning algorithms for scoliosis screening using back images," *Communications biology*, vol. 2, no. 1, pp. 1-8, 2019.
- [48] X. Guo, S. Xu, Y. Wang, J. P. Y. Cheung, and Y. Hu, "Prediction model of scoliosis progression based on deep learning," in *Cyberspace Data and Intelligence, and Cyber-Living, Syndrome, and Health*: Springer, 2019, pp. 431-440.
- [49] R. Korez, B. Ibragimov, B. Likar, F. Pernuš, and T. Vrtovec, "A framework for automated spine and vertebrae interpolation-based detection and model-based

- segmentation," *IEEE transactions on medical imaging*, vol. 34, no. 8, pp. 1649-1662, 2015.
- [50] E. Magnide *et al.*, "Automatic bone maturity grading from EOS radiographs in Adolescent Idiopathic Scoliosis," *Computers in Biology and Medicine*, vol. 136, p. 104681, 2021.
- [51] J. Li, S. Li, Z. Yang, T. Wu, and Y. Hu, "An Automatic Scoliosis Diagnosis Platform Based on Deep Learning Approach," in *2022 4th Asia Pacific Information Technology Conference*, 2022, pp. 215-223.
- [52] A. Y. Ha *et al.*, "Automating Scoliosis Measurements in Radiographic Studies with Machine Learning: Comparing Artificial Intelligence and Clinical Reports," *Journal of Digital Imaging*, pp. 1-10, 2022.
- [53] Y. Tu, N. Wang, F. Tong, and H. Chen, "Automatic measurement algorithm of scoliosis Cobb angle based on deep learning," in *Journal of Physics: Conference Series*, 2019, vol. 1187, no. 4: IOP Publishing, p. 042100.
- [54] N. A. Makhdoomi *et al.*, "Development of Scoliotic Spine Severity Detection using Deep Learning Algorithms," in *2022 IEEE 12th Annual Computing and Communication Workshop and Conference (CCWC)*, 2022: IEEE, pp. 0574-0579.
- [55] M. Fraiwan, Z. Audat, L. Fraiwan, and T. Manasreh, "Using deep transfer learning to detect scoliosis and spondylolisthesis from x-ray images," *Plos one*, vol. 17, no. 5, p. e0267851, 2022.
- [56] W. Caesarendra, W. Rahmaniari, J. Mathew, and A. Thien, "Automated Cobb Angle Measurement for Adolescent Idiopathic Scoliosis Using Convolutional Neural Network," *Diagnostics*, vol. 12, no. 2, p. 396, 2022.
- [57] R. Hamzah, N. Sabri, S. K. N. A. Rahim, N. Jamil, and Z. Ibrahim, "Improving the Classification of Scoliosis on Radiographic Image using the AdaBoost Ensemble Model," *Journal of Positive School Psychology*, vol. 6, no. 3, pp. 8407–8414-8407–8414, 2022.
- [58] N. Sabri, H. N. A. Hamed, Z. Ibrahim, and K. Ibrahim, "A Comparison between Average and Max-Pooling in Convolutional Neural Network for Scoliosis Classification," *International Journal*, vol. 9, no. 1.4, 2020.
- [59] A. A. Abdullah, A. Yaakob, and Z. Ibrahim, "Prediction of spinal abnormalities using machine learning techniques," in *2018 International conference on computational approach in smart systems design and applications (ICASSDA)*, 2018: IEEE, pp. 1-6.

- [60] A. Ha *et al.*, "Automatic Extraction of Skeletal Maturity from Whole Body Pediatric Scoliosis X-rays Using Regional Proposal and Compound Scaling Convolutional Neural Networks," in *2020 IEEE International Conference on Bioinformatics and Biomedicine (BIBM)*, 2020: IEEE, pp. 996-1000.
- [61] G. A. Lein, N. S. Nechaeva, G. M. Mammadova, A. A. Smirnov, and M. M. Statsenko, "Automation analysis X-ray of the spine to objectify the assessment of the severity of scoliotic deformity in idiopathic scoliosis: A preliminary report," *Pediatric Traumatology, Orthopaedics and Reconstructive Surgery*, vol. 8, no. 3, pp. 317-326, 2020.
- [62] V. Miglani and M. Bhatia, "Skin lesion classification: A transfer learning approach using efficientnets," in *International Conference on Advanced Machine Learning Technologies and Applications*, 2020: Springer, pp. 315-324.
- [63] S. Wang, S. Huang, and L. Wang, "Spinal curve guide network (SCG-Net) for accurate automated spinal curvature estimation," in *International Workshop and Challenge on Computational Methods and Clinical Applications for Spine Imaging*, 2019: Springer, pp. 107-112.
- [64] P. Chen, Z. Zhou, H. Yu, K. Chen, and Y. Yang, "Computerized-Assisted Scoliosis Diagnosis Based on Faster R-CNN and ResNet for the Classification of Spine X-Ray Images," *Computational and Mathematical Methods in Medicine*, vol. 2022, 2022.
- [65] M. Raihan-Al-Masud and M. R. H. Mondal, "Data-driven diagnosis of spinal abnormalities using feature selection and machine learning algorithms," *Plos one*, vol. 15, no. 2, p. e0228422, 2020.
- [66] F. Galbusera, G. Casaroli, and T. Bassani, "Artificial intelligence and machine learning in spine research," *JOR spine*, vol. 2, no. 1, p. e1044, 2019.
- [67] A. Amin, M. Abbas, and A. A. Salam, "Automatic Detection and classification of Scoliosis from Spine X-rays using Transfer Learning," in *2022 2nd International Conference on Digital Futures and Transformative Technologies (ICoDT2)*, 2022: IEEE, pp. 1-6.
- [68] W. Caesarendra, W. Rahmaniar, J. Mathew, and A. Thien, "AutoSpine-Net: Spine detection using convolutional neural networks for Cobb angle classification in adolescent idiopathic scoliosis," in *Proceedings of the 2nd International Conference on Electronics, Biomedical Engineering, and Health Informatics*, 2022: Springer, pp. 547-556.

- [69] D. P. Kingma and J. Ba, "Adam: A method for stochastic optimization," *arXiv preprint arXiv:1412.6980*, 2014.
- [70] M. Abadi *et al.*, "Tensorflow: Large-scale machine learning on heterogeneous distributed systems," *arXiv preprint arXiv:1603.04467*, 2016.